Combining the entropy-scaling concept and cubic- or SAFT equations of state for modelling thermal conductivities of pure fluids

Aghilas Dehlouz, Jean-Noël Jaubert, Guillaume Galliero, Marc Bonnissel, Romain Privat

International Journal of Heat and Mass Transfer 196 (2022) 123286

Contents lists available at ScienceDirect

International Journal of Heat and Mass Transfer

journal homepage: www.elsevier.com/locate/hmt

Combining the entropy-scaling concept and cubic- or SAFT equations of state for modelling thermal conductivities of pure fluids

Aghilas Dehlouz[a,b], Jean-Noël Jaubert[a,*], Guillaume Galliero[c], Marc Bonnissel[b], Romain Privat[a]

[a] Université de Lorraine, École Nationale Supérieure des Industries Chimiques, Laboratoire Réactions et Génie des Procédés (UMR CNRS 7274), 1 rue Grandville, 54000 Nancy, France
[b] Gaztransport & Technigaz (GTT), 1 route de Versailles, 78470 Saint-Rémy-lès-Chevreuse, France
[c] Université de Pau et des Pays de l'Adour, E2S UPPA, CNRS TotalEnergies, LFCR UMR 5150, Pau, France

ARTICLE INFO

Article history:
Received 4 May 2022
Revised 30 June 2022
Accepted 24 July 2022
Available online 5 August 2022

ABSTRACT

The transport properties of a fluid show a complex dependence with temperature and pressure due to the combination of different phenomena occurring at the microscopic scale. The entropy scaling concept aims at describing this complex behavior by expressing reduced transport properties as one-variable functions of the Tv-residual entropy, a thermodynamic quantity that can be straightforwardly estimated with an equation of state (EoS). In this work, a reformulated version of Rosenfeld's original entropy scaling approach is proposed in order to calculate the thermal conductivities of pure fluids. A specifically developed reduced thermal conductivity expression was correlated to a function of the Tv-residual entropy that was recently proposed by our group to correlate viscosities and self-diffusion coefficients. The thermodynamic properties involved in the definition of the entropy-scaling variables (that are the residual entropies, densities, heat capacities) were estimated with either the *I*-PC-SAFT or the *tc-PR* equations of state (EoSs) thus leading to the definition of two different models. Each of them was validated against a large database of around 90,000 experimental thermal conductivities encompassing liquid, gas and supercritical states for 119 chemical species belonging to 11 chemical families such as n-alkanes, alkenes, alcohols, HFC-CFC etc. For each model, component-specific, chemical-family specific and universal parameters were proposed. Working with the *I*-PC-SAFT and *tc*-PR EoSs, the obtained MAPEs (Mean Absolute Percent Errors) are respectively 3.3% and 3.4% when the model parameters are considered as component-specific, 9.7% and 5.6% when they are selected as chemical-family specific meanwhile they are 11.2% and 9.2% when they are assumed to be universal.

1. Introduction

Advection and conduction (or diffusion), i.e. convection, are two mechanisms governing heat transfers in fluids. In the absence of advection, thermal energy is transferred at the microscopic scale through displacements and collisions of particles (molecules, atoms, electrons). The thermal conductivity, often denoted λ, is the corresponding transport property which characterizes the ability of a material to transfer thermal energy by conduction and is related to the heat flux through phenomenological laws such as Fourier's law. This property is essential for designing industrial operation units in which heat transfers have a central place (e.g., heat exchangers) [1] thus justifying the need for efficient methods to estimate it. There exist currently various empirical or semi-empirical methods that allow its estimation with an affordable time-efficiency/precision compromise:

- Empirical correlations [2] expressing the thermal conductivity as a function of temperature or density for a given range of fluid conditions
- Models inspired from cubic equations of state (EoS) and taking benefit of the geometric similitude observed between the (P, v, T) and the (T, λ, P) behaviors of a pure fluid [3], where P represents the pressure, T is the temperature and v is the molar volume.
- Approaches based on a dimensional analysis [4] that correlate the thermal conductivity of a fluid to other fluid properties, e.g., temperature, critical constants, molecular weight etc.

* Corresponding author at: Universite de Lorraine ENSIC, France.
E-mail addresses: jean-noel.jaubert@univ-lorraine.fr (J.-N. Jaubert), romain.privat@univ-lorraine.fr (R. Privat).

https://doi.org/10.1016/j.ijheatmasstransfer.2022.123286

- Corresponding-state methods [5] that predict the thermal conductivity of a fluid from the mere knowledge of its critical constants, acentric factor, molecular weight and ideal gas heat capacity.
- The scheme by Assael and Dymond [6] in which the thermal conductivity is defined as a function of the close-packed volume V_0, the temperature and the number of carbon atoms.
- The Friction Theory [7] in which the thermal conductivity is correlated to the residual entropy stemming from an EoS.
- The entropy scaling approach [8–19] which relates the reduced transport property (the dimensionless thermal conductivity) to the Tv-residual entropy.

In addition to the above-mentioned approaches, it is worth recalling that the kinetic theory of gases [20], which relates transport properties to the dynamics of binary collisions, remains one of the most physically-sound approaches used today in gases. In particular, it can be used to ensure a correct zero density limit for approaches that does not provide direct expressions for the transport property itself but estimate a residual transport property; this is, e.g., the case with the friction theory [7] or with models based on the entropy scaling concept [18]. However, it is only applicable to dilute-gas states and suffers from not considering the multiple internal degrees of freedom possessed by polyatomic molecules that strongly impact the thermal conductivities of dilute gases. It is well-acknowledged indeed that the derivation of an accurate and physically-based model for thermal conductivity estimation should rely on a comprehensive understanding of the actual mechanisms associated with the different modes of energy transfer in polyatomic molecules through the internal translational, rotational and vibrational contributions.

Despite considerable efforts to develop and extend the scope of the above-mentioned methods, a model to describe transport properties behavior, stemming from rigorous theory applicable to all fluid states and all pure compounds regardless of their chemical structure is still expected by the industrial and academic communities. We are however convinced that the entropy scaling concept [8] is a remarkably robust concept enabling to approach this objective. It can be applied to the modelling of the following three transport properties: the dynamic viscosity, the mass diffusion coefficient and the thermal conductivity. In brief, the approach is based on the existence of a functional relationship between a reduced (i.e., dimensionless) expression of the transport properties and the Tv-residual entropy, this latter quantity revealing information about the internal structure of fluids. Note that "Tv-residual entropy", denoted $s_{\mathrm{Tv-res}}$, refers here to the departure entropy between the real fluid and the corresponding perfect gas having the same temperature and molar volume as the real fluid. The reduced transport property is defined as the ratio of a real transport property (e.g., a thermal conductivity) and a reference property having the same unit.

This concept was originally developed by Rosenfeld [8] who worked on simple fluids and proposed different correlations applicable either to liquid or gaseous components. Since Rosenfeld's pioneering work, several studies investigated this concept to assess its range of applicability or improve it. A literature review on Rosenfeld's proposal application to real fluids leads to the following observations:

- The relation between the transport properties, specifically the thermal conductivity, and the Tv-residual entropy is not universal; it depends on the considered component.
- A systematic divergence of the transport properties is present at low-density states, regardless of the transport property considered (starting generally from $s_{\mathrm{Tv-res}} > -0.5$).
- By defining an appropriate reference property following Rosenfeld's proposition, the monovariable relationship between the Tv-residual entropy and the transport properties exists over the entire fluid region.

After reviewing the main advances in the modelling of thermal conductivity through the entropy scaling concept, this study proposes a new approach relying on this theory to model the thermal conductivity of a pure fluid in any physical state condition (liquid, gas or supercritical) through a unique equation. Equations of state are used to estimate thermodynamic fluid properties that are the density, heat capacity at constant volume and $s_{\mathrm{Tv-res}}$. Two versions of this correlation are proposed, one using a SAFT-type EoS, namely the *I*-PC-SAFT[21] model, and the second one using a cubic EoS, the *translated* [22,23]-*consistent* [24,25] Peng-Robinson (*tc*-PR [26]) model.

The method proposed here has been successfully applied to a comprehensive database of around 90,000 experimental thermal conductivity data involving 119 chemical components. Different model parametrizations are then proposed: model parameters can be chosen (i) component specific, (ii) chemical-family specific (i.e., identical for all the species of a same chemical family) or (iii) universal (i.e., a unique set of parameters is used for all components without restriction). These three approaches make it possible to select the appropriate approach depending on the situation. Therefore, for estimating the thermal conductivity of a given component in given conditions of temperature and pressure:

- the highest accuracy is obviously obtained with component-specific parameters; this approach can be used provided experimental data are available for the concerned molecule.
- If it is not the case, chemical-family specific parameters can be used otherwise, provided the component belongs to one of the chemical family considered in this study.
- If neither of the two approaches mentioned above can be used (no experimental data are available or the given species does not belong to a specific chemical family), universal parameters can be used to calculate the thermal conductivity with reasonable accuracy.

2. Theoretical background

2.1. Modelling the thermal conductivity of fluids

Various modelling approaches of the thermal conductivity assume that this property aggregates three independent contributions [27]:

$$\lambda(\rho,T) = \lambda_0(T) + \Delta\lambda_c(\rho,T) + \Delta\lambda(\rho,T) \quad (1)$$

Where

- $\lambda(\rho,T)$ is the thermal conductivity of the real fluid which depends on the temperature T and the density ρ.
- $\lambda_0(T) = \lambda(0,T)$ is the zero-density (or the dilute-gas) contribution which only depends on the temperature. In addition, only two-body interactions are considered in this term.
- $\Delta\lambda_c(\rho,T)$ represents the critical enhancement contribution resulting from the long-range density fluctuations appearing near the critical point [28].
- $\Delta\lambda(\rho,T)$ is a residual contribution accounting for all other effects. It reveals phenomena arising at moderate to elevated densities including many-body collisions, molecular-velocity correlations, and collisional transfers [27].

A similar decomposition can be used for the viscosity. Nevertheless, the following significant differences exist between the two transport properties [9]:

- While the viscosity critical enhancement is asymptotic and is restrained to a close region in the vicinity of the critical point,

the thermal conductivity enhancement is significant over a larger range of fluid conditions. It has to be noted that despite the considerable effort provided to model the critical enhancement of the thermal conductivity [29–31], an efficient and broadly applicable theory or model is still lacking. For this reason, this phenomenon was not considered in the present study and the experimental data points in the vicinity of the critical point were discarded (see section III for more details on the selection of the experimental data).

- While the viscosity of gases is mainly governed by the transfer of a translational energy, thermal conductivity of polyatomic gases is also considerably affected by vibrational and rotational degrees of freedom. Consequently, whereas dilute-gas contributions for viscosity can be limited to expressions accounting for translational movement using, e.g., the Chapman-Enskog model, this is not a reasonable assumption for thermal conductivity.

To model $\lambda_0(T)$, the Chapman-Enskog equation for thermal conductivity, given by Eq. (2), is insufficient and needs to be completed with rotational and vibrational contributions.

$$\lambda^{CE} = \frac{75}{64}\sqrt{\frac{k_b T}{m_0 \pi}}\frac{1}{\sigma^2 \Omega^{(2,2)*}} \tag{2}$$

In Eq. (2), k_b is the Boltzmann constant, m_0 is the molecular mass, σ and $\Omega^{(2,2)*}$ are the Lennard-Jones characteristic collision diameter and the Lennard-Jones collision integral respectively.

Empirically, Eucken [2,32] proposed to decompose the dilute-gas contribution of the thermal conductivity into two independent parts: a translational contribution (λ_{tr}) and an additional part (λ_{int}) characterizing the internal energy transferred through rotational and vibrational degrees of freedom (see Eqs. 3 and 4).

$$\lambda_0 = \lambda_{tr} + \lambda_{int} \tag{3}$$

With:

$$\begin{cases} \lambda_{tr} = \eta \times f_{tr} \times c_{v,tr} \\ \lambda_{int} = \eta \times f_{int} \times c_{v,int} \end{cases} \tag{4}$$

η is the dynamic viscosity of the dilute gas, $c_{v,tr} = \frac{3}{2}R$ and $c_{v,int}$ are the translational and internal contributions to the specific heat capacity at constant volume (c_v), respectively. These two terms are making up to total molar heat capacity: $c_v = c_{v,tr} + c_{v,int}$. The factors f_{int} and f_{tr} are usually fixed to 1 and $\frac{5}{2}$ [2] although those values are still open to question. Therefore, some authors such as Chapman and Cowling [20] proposed to modify Eucken's formula assuming that the transport of internal energy is governed by a diffusion mechanism. This assumption led to the introduction of the self-diffusion coefficient D_{self} in the definition of the factor f_{int} ($f_{int} = \rho D_{self}/\eta$) thus leading to:

$$\lambda_{int} = \rho D_{self} c_{v,int} \tag{5}$$

Eq. (3) can thus be rewritten as:

$$\lambda_0 = \lambda_{tr} + \rho D_{self} c_{v,int} \tag{6}$$

2.2. Application of the entropy scaling concept to thermal conductivity: key advances

The entropy scaling concept is based on the relation between the transport properties (reflecting the dynamic behavior of molecules at the microscopic scale) and the Tv-residual entropy (providing information on the structure of the fluid). The Tv-residual entropy of a fluid can be estimated from an EoS in a straightforward manner from the following expression:

$$\begin{cases} s_{Tv-res} = s_{real}(T,v) - s_{perfect\ gas}(T,v) = -\left(\frac{\partial a_{Tv-res}}{\partial T}\right)_v \\ \text{with}: \quad a_{Tv-res} = -\int_{+\infty}^{v}\left[P(T,v) - \frac{RT}{v}\right]dv \end{cases} \tag{7}$$

where s_{Tv-res} is the Tv-residual entropy, s_{real} is the actual molar entropy of the real fluid (in a liquid, gas or supercritical state), $s_{perfect\ gas}$ is the perfect-gas entropy (note that the term perfect gas is preferred to ideal gas following the recommendations of Privat et al.[33]), R is the universal gas constant, a_{Tv-res} is the Tv-residual molar Helmholtz energy, and $P(T,v)$ is the EoS. As mentioned in the introduction, the existence of a simple relation between s_{Tv-res} and transport properties was proposed by Rosenfeld when working on simple theoretical fluids at dense states. He pointed out that reduced (i.e., dimensionless) expressions of the viscosity, self-diffusion coefficient [34] and thermal conductivity [8] can be formulated as monovariable functions of the Tv-residual entropy. To reduce the transport properties, Rosenfeld divided the actual transport properties by a dimensionally-equivalent quantity depending on fluid temperature and density which was defined from elementary kinetic-theory considerations. Concerning the thermal conductivity, the corresponding reduced property was defined as:

$$\tilde{\lambda} = \frac{\lambda_{real}}{\lambda_{reference}} = \frac{\lambda_{real}}{\rho_N^{\frac{2}{3}} k_b \sqrt{k_b T / m_0}} \tag{8}$$

where $\rho_N = \rho N_a$ is the molecular density (product of molar density ρ and Avogadro's number N_a) and m_0 is the molecular weight. According to the entropy-scaling theory, the reduced thermal conductivity and the residual entropy are connected through a simple relation denoted: $\tilde{\lambda} = f(s_{Tv-residual})$. Doing so, the actual property (λ_{real}) is obtained from:

$$\lambda_{real} = \lambda_{reference} \times f(s_{Tv-residual}) \tag{9}$$

As pointed out by Rosenfeld [8], this approach, that combines simplicity and broad applicability, is more a semi-quantitative model than a real theory. On one hand, it offers many advantages:

- it involves easily accessible and straightforwardly calculable quantities (the molar density, i.e. the inverse of the molar volume and the Tv-residual entropy are obtained from an EoS),
- it can be applied to the three transport properties (viscosity, self-diffusion coefficient and thermal conductivity).

On the other hand, the application of the concept to real substances suffers of several deficiencies:

- A systematic divergence at low density,
- The non-universality of the function f involved in Eq. (9) (the mathematical expression of f and/or the numerical values of the function parameters are component specific)

In the literature, previous studies aimed at improving the modelling of thermal conductivity based on entropy scaling considered the following directions: (i) modification of the mathematical formulation of function f in Eq. (9) in order to extend the model range of applicability and tend to a universal behavior, (ii) search for a proper expression of the reference property $\lambda_{reference}$ (appearing in the denominator of the reduced thermal conductivity in Eq. (8)) with the ambition to improve the description of low-density data. In particular, several works proposed to specifically account in this term for the translational, rotational, vibrational and internal degrees of freedom characterizing polyatomic gases.

Inspired by Novak's proposal [35,36] and the successful use of the Chapman-Enskog equation [20] as the reference property for reducing the dynamic viscosity [37,38], Hopp and Gross [10] proposed a new expression for the reference thermal conductivity where (i) both the segment diameter and the pair energy parameter (involved in Eq. (2)) were replaced by the corresponding PCP-SAFT EoS parameters and; (ii) the molecular mass m_0 was divided by the segment number m. However, in order to take account for

the rotational and vibrational degrees of freedom in polyatomic gases, Hopp and Gross added a correction term to the Chapman-Enskog equation: $\lambda_{ref} = \lambda^{CE} + \lambda_{int}$. They introduced a temperature-dependent correlation for λ_{int} and used an empirical factor ("activation function") of the form $e^{-(s_{Tv-res}/s^c_{Tv-res})}$ to make λ_{int} exist at low density only. Model parameters were estimated from the group-contribution concept to make their model predictive [12]. Although the model offers accurate predictions of thermal conductivity for polyatomic molecules in the low-density region, the proposed temperature-dependent correlation for λ_{int} remains unsatisfactory for substances showing a small number of internal degrees of freedom (e.g., Xenon, Nitrogen). As an alternative, Hopp et al. [11] proposed to introduce both a temperature and density dependency in the self-diffusion coefficient as well as the total molar isochoric heat capacity in the expression of λ_{int} (see Eq. (5)). The description of the thermal conductivities of simple gases and diatomic fluids was thus improved considerably even if the use of Eq. (5) requires the knowledge of the corresponding self-diffusion coefficient.

Most of the studies dealing with the application of entropy scaling to thermal conductivities concern refrigerants and their mixtures involved in current cooling systems. In this context, several authors followed a similar methodology for defining the reference thermal conductivity. As an example, in their study on HFC and HFO, Liu et al. [17] used the Eucken's approach (see Eqs. (3) and (4)) to define λ_{ref} but replaced the translational contribution by the Chapman-Enskog relation reported in Eq. (2) and correlated f_{int} as a temperature-dependent polynomial for each fluid.

In order to predict the thermal conductivities of hydrocarbon mixtures and fuels, Rokni et al. [13,14] proposed to use a pseudo-component approach where the mixture is represented as a unique substance made up of a hydrocarbon chain. Their model is applicable to dense states and thus, ignores the λ_{int} contribution to the reference thermal conductivity. The reference property used for the reduction is based on the Chapman-Enskog relation ($\lambda_{ref} = \lambda_{tr} = \lambda^{CE}$); the diameter σ and energy ε parameters are taken as those of the defined pseudo component, while the molecular mass m_0 of the pseudo is divided by its chain length.

A different strategy was followed by Bell for approaching the zero-density limit [39]. He fixed λ_{ref} by referring to Rosenfeld's scaling and confirmed this choice by referring to the isomorph theory [40] which uses the same reference thermal conductivity. However, he introduced an empirical correction consisting in multiplying Rosenfeld's λ_{ref} by a factor $(-\tilde{s}_{Tv-res})^{2/3}$ that "does not break that scaling while simultaneously fixing the dilute gas divergence"[18]. Highlighted by Galliero [41] as having a positive impact on the ability of correlating the thermal conductivity at low densities, Bell replaced the actual thermal conductivity appearing in the numerator of Eq. (8) by a "residual" thermal conductivity obtained by subtracting the zero-density value to the actual one. Therefore, in his approach, Bell correlated a residual conductivity to the Tv-residual entropy.

While offering generally a better modelling of thermal conductivities and a better characterization of the low-density limit, Bell's approach leads nevertheless to significant deviations at low density [42]. Recently, this approach was applied to refrigerants and their mixtures by including a critical enhancement contribution in the definition of the residual conductivity. The latter contribution was estimated using the Olchowy and Sengers model [29] and the dilute-gas contribution was calculated using REFPROP 10.0 software package [43]. Following Liu et al. proposal [17], a component specific parameter was used to normalize the T-v-residual entropies values and to fit the considered experimental data to a single curve.

2.3. A new approach

Despite all the efforts devoted to improve the entropy scaling concept in the last few years, its optimal formulation is still open to question. As shown in Fig. 1-A, Rosenfeld's proposal was found to be valid at dense state but shows a diverging behavior at low density. As pointed by Dzugutov [44], the monovariable relationship observed at dense state ($\tilde{s}_{Tv-res} < -0.5$) can be ascribed to the strong correlation between the dynamical behavior of molecules, which is reflected by transport properties, and the structural relaxations, which are proportional to the number of accessible configurations per atom, and therefore, to the exponential of entropy (according to Boltzmann's formula). By increasing with density and thus with the absolute Tv-residual entropy, this strong correlation overrides the effect of the reduction and makes it barely needed at dense states. As the density decreases and as molecular kinetics plays a more prominent role, the correlation between the transport property and the residual entropy becomes more complex and only a reduced transport property can be correlated to the residual entropy. It is worth recalling that the use of the Chapman-Enskog (CE) equations for expressing the reference transport properties (thermal conductivity in the present case) fixes partially the low-density divergence by inducing a well-defined limit at low density. However, this choice is not fully satisfactory because:

- The entropy scaling concept has the ambition to be applicable to the entire fluid region while the CE relation only describes the dilute gas domain. A direct consequence is the appearance of scattered experimental data at low and moderate density conditions in the reduced thermal conductivity versus reduced residual entropy plot. This scattering phenomenon is particularly visible with argon in Fig. 1-B. This component was selected as an illustrative example because the CE relation is acknowledged to be a good approximation to describe the thermal conductivity of monoatomic gases.
- This approach requires the preliminary knowledge of additional component-specific parameters, namely: the collision diameter and the molecular attraction parameter.
- In the case of the thermal conductivity, the CE relation does not account for the rotational and vibrational degrees of freedom characterizing polyatomic molecules so that a strong scattering of experimental data due to the nature of the reduction (i.e. independent from the experimental uncertainties) is observed in Fig. 1-B for polyatomic molecules like methane, ethane and n-hexane at $\tilde{s}_{Tv-res} > -2$.

Such weaknesses persist if one switches to a residual approach (i.e., when the actual thermal conductivity is replaced by a residual conductivity obtained by subtracting the zero-density contribution to the actual property).

Based on the results obtained when working on the viscosity of simple fluids at dense states, Rosenfeld [8,34] modelled the relation between the reduced transport property and the Tv-residual entropy with an exponential function. This empirical choice was convenient since it can be observed that experimental data align along straight lines in a semi log scale in a large range of dense-fluid conditions. For dilute gases, he proposed a power law relation based on Enskog's results [8]. Inspired by these results, a new variable, noted X_{ES}, depending on the Tv-residual entropy was recently introduced by our group [46] with the ambition to reproduce simultaneously the experimental data at low and high-density:

$$X_{ES} = -\left(\frac{s_{Tv-res}}{s^c_{Tv-res}}\right) - ln\left(\frac{s_{Tv-res}}{s^c_{Tv-res}}\right) = -\left(\frac{\tilde{s}_{Tv-res}}{\tilde{s}^c_{Tv-res}}\right) - ln\left(\frac{\tilde{s}_{Tv-res}}{\tilde{s}^c_{Tv-res}}\right) \quad (10)$$

In Eq. (10), $\tilde{s}^c_{Tv-res}$ is the critical value of the reduced molar entropy $\tilde{s}_{Tv-res} = \frac{s_{Tv-res}}{R}$. It can be noted that the 1st term is dominant

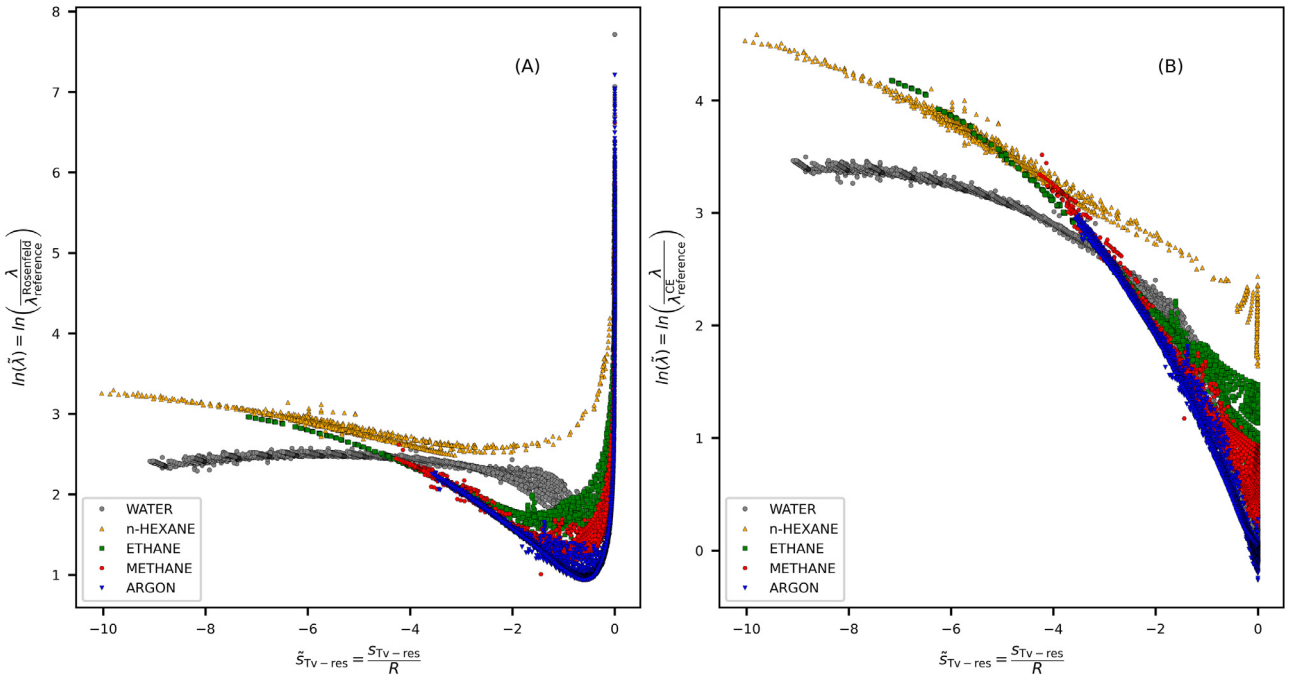

Fig. 1. Plot of the experimental reduced thermal conductivity as a function of the reduced Tv-residual entropy using the *I*-PC-SAFT EoS. Subplot (A): using Rosenfeld's original reduction. Subplot (B): using the Chapman-Enskog relation for defining the reference thermal conductivity (data source: Dortmund Data Bank [45]; the data selection procedure is described in section III).

in dense-fluid condition while the 2nd term dominates at low density. Remarkably, the X_{ES} variable makes it possible:

- To avoid the low-density divergence and to reach a well-characterized zero-density limit when the reduced transport property is defined from Rosenfeld's reference term,
- To achieve a quasi-universal behavior at low densities for both the viscosity and the self-diffusion coefficient [47],
- To obtain more closely packed curves since the $\frac{\tilde{s}_{Tv-res}}{\tilde{s}^{c}_{Tv-res}}$ ratio was found to take similar values for different chemical species and was found to slightly depend on the selected EoS.

Our paper devoted to viscosity [46] underlined that numerical values of s_{Tv-res} could differ significantly from one EoS to another. Although dividing the Tv-residual entropy by its value at the critical point strongly attenuates this difference, we found necessary to add a temperature-dependent term in the mathematical expression of the X_{ES} variable (see Eq. (11)) when the *tc*-PR EoS is used. This patch, specific to the *tc*-PR EoS and only needed at very high temperatures ($4T_c < T < 8T_c$, where T_c denotes the critical temperature of the fluid) was introduced to keep the same mathematical expression of the X_{ES} variable (see Eq. (10)) regardless of the EoS used to estimate the density, residual isochoric heat capacity and residual entropy: it is indeed enough to select $f_{corr}(T) = 1$ in Eq. (11) when one works with the *I*-PC-SAFT EoS.

To sum up, for heavy molecules for which the temperature domain $T > 4T_c$ is not of practical interest, a null α value is selected in Eq. (11). Otherwise, for light molecules (having a low T_c) such as Ar, N_2 or Krypton for which experimental thermal conductivities are available at high reduced temperatures ($4T_c < T < 8T_c$) a non-zero coefficient was selected. The influence of this correction is illustrated with Argon in Fig. 16 of Appendix A.

$$\begin{cases} X^{corrected}_{ES-tc-PR} = -\left(\frac{\tilde{s}_{Tv-res}}{\tilde{s}^{c}_{Tv-res}}\right) - \ln\left(\frac{\tilde{s}_{Tv-res}}{\tilde{s}^{c}_{Tv-res}} \times f_{corr}(T)\right) \\ f_{corr}(T) = 1 + \alpha\left(\frac{T-T_c}{T_c}\right)^3 \end{cases} \quad (11)$$

It is worth noting that as long as a given equation of state qualitatively reproduces the temperature and pressure dependence of the Tv-residual entropy regardless of the fluid conditions (as the *I*-PC-SAFT EoS does), it is not necessary to applies this patch.

In order to observe how the entropy scaling relation is affected by the change of variable $\tilde{s}_{Tv-res}$ to X_{ES}, Fig. 2 illustrates the application of the entropy scaling concept defined by the general relation $\tilde{\lambda} = \frac{\lambda}{\lambda_{ref}} = f(X_{ES})$ to 5 molecules (water, argon, methane, ethane and n-hexane). Subplot A in Fig. 2 shows the curves obtained using Rosenfeld's definition for λ_{ref} while in subplot B, the Chapman-Enskog relation was used instead.

Fig. 2 demonstrates that both reductions provide an acceptable scaling at high densities (i.e., at $X_{ES} < 0$). The use of the original Chapman-Enskog relation (not corrected to account for the many degrees of freedom possessed by polyatomic molecules) for defining λ_{ref} results in a scattering of the experimental data in low-density conditions (see the case of n-hexane and ethane at $X_{ES} \geq 0$ in Fig. 2-B). For the Argon case shown in Fig. 2-B, for which the contribution of the vibrational and rotational degrees of freedom to the thermal conductivity is negligible, a horizontal asymptote appears due to the capacity of the CE relation to satisfactorily reproduce the thermal conductivity of simple gases at low density and thus making $\ln(\tilde{\lambda})$ tends to 0. However, since the CE relation is not suitable for moderately dense gases and/or supercritical fluid conditions, data scatter is visible at $X_{ES} \geq 0$.

The use of Rosenfeld's reduction approach, $\tilde{\lambda} = \lambda/\lambda^{Rosenfeld}_{ref}$, also leads to data scatter for molecules that possess vibrational and rotational degrees of freedom while data align along a master curve when these degrees of freedom become negligible (see the case of argon at $X_{ES} \geq 0$ in Fig. 2-A).

To account for these specific phenomena exhibited by polyatomic molecules (i.e., the transfer of vibrational energy during molecules collision) and thus to extend the scope of the entropy scaling concept to such molecules, it was decided to test out Eucken's approach along with the Chapman and Cowling assumption (see Eq. (6)) to combine (i) a corrected macroscopic reduction based on Rosenfeld's proposal (see Eq. (12)) and (ii) a microscopic corrected reduction based on the Chapman-Enskog relation

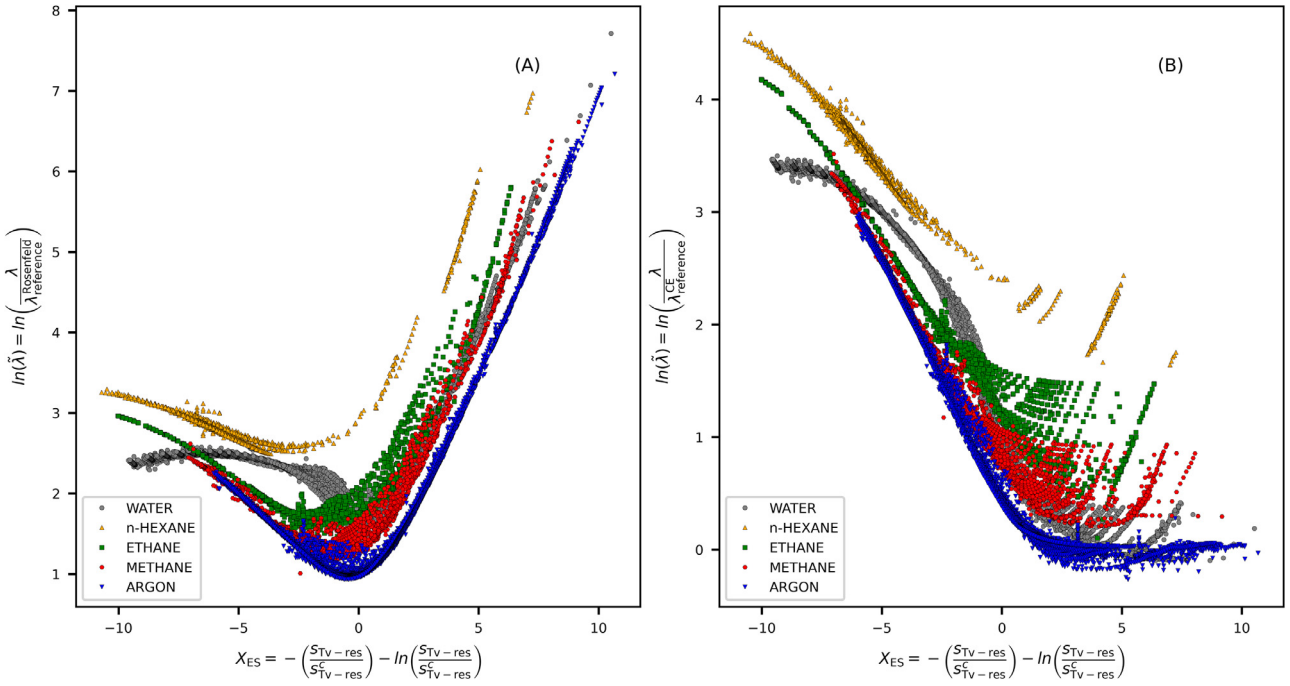

Fig. 2. Plot of the experimental reduced thermal conductivity as a function of the proposed entropy variable X_{ES} using the *I*-PC-SAFT EoS. Subplot (A): the reduced thermal conductivity defined according to Rosenfeld. Subplot (B): The Chapman-Enskog relation is used to define the reference thermal conductivity.

Table 1
Expressions of the reference thermal conductivity, corrected to account for the internal degrees of freedom encountered in polyatomic molecules

Macroscopic corrected reduction (Eq. 12)	Microscopic corrected reduction (Eq. 13)
Where: $\begin{cases} \lambda_{ref}^{Rosenfeld} = \rho_N^{\frac{2}{3}} k_b \sqrt{k_b T / m_0} \\ D_{self,ref}^{Rosenfeld} = \rho_N^{-\frac{1}{3}} \sqrt{k_b T / m_0} \\ g(\rho) = e^{-(\rho/\rho_c)} \end{cases}$	Where: $\begin{cases} \lambda_{ref}^{CE} = \frac{75}{64} \sqrt{\frac{k_b T}{m_0 \pi}} \frac{1}{\sigma^2 \Omega^{(2,2)*}} \\ D_{self,ref}^{CE} = \frac{3}{8\rho_N} \sqrt{\frac{k_b T}{m_0 \pi}} \frac{1}{\sigma^2 \Omega^{(1,1)*}} \\ g(\rho) = e^{-(\rho/\rho_c)} \end{cases}$

(see Eq. (13)).

$$\lambda_{ref}^{Rosenfeld,intDoF} = \lambda_{ref}^{Rosenfeld} + g(\rho)\rho D_{self,\ ref}^{Rosenfeld} c_v^{real} \tag{12}$$

$$\lambda_{ref}^{CE,\ intDoF} = \lambda_{ref}^{CE} + g(\rho)\rho D_{self,ref}^{CE} c_v^{real} \tag{13}$$

Both of the investigated reductions are reported in Table 1. In such a table c_v^{real} is the molar isochoric heat capacity defined as $c_v^{real} = c_v^{res} + c_v^0$. The residual specific heat capacity at constant volume c_v^{res} was obtained from the considered EoS (the *I*-PC-SAFT or the *tc*-PR EoS) while the ideal gas contribution c_v^0 was estimated from the correlations provided by the Design Institute for Physical Properties (DIPPR) [48]. Because of the importance of the reference term, we believe it is important to provide information on the ability of the two EoSs to predict heat capacities. Our recent studies on these 2 EoSs in which the heat capacities of 890 pure components were predicted lead to the conclusion that the MAPE on heat capacities returned by the *tc*-PR and *I*-PC-SAFT EoSs are respectively 2.53% [49] and 4.10% [50] what is considered acceptable. ρ is the molar density in $mol \cdot m^{-3}$ and ρ_N is the molecular density in m^{-3}. σ and $\Omega^{(*,*)*}$ are the Lennard-Jones characteristic collision diameter and the Lennard-Jones collision integral, respectively. In this paper, the collision integrals $\Omega^{(1,1)*}$ and $\Omega^{(2,2)*}$ were estimated using Neufeld's empirical equation [51] while both the Lennard-Jones characteristic collision diameter (σ) and the molecular attraction parameter (ε) required to estimate $\Omega^{(1,1)*}$ and $\Omega^{(2,2)*}$ were taken from reference [52]. In both reductions reported in Table 1, the c_v^{real} is considered rather than c_v^0 in order to ensure a better applicability of the entropy scaling relation in the whole fluid domain. In addition, while Eq. (6) involves an "internal" heat capacity defined as $c_{v,int} = c_v - c_{v,tr}$, it was decided to ignore the translation term ($c_{v,tr}$) since (i) this term is generally approximated by the fixed value of $\frac{3}{2}R$ which is only valid for simple gases in the ideal gas limit and (ii) neglecting this constant value does not change the qualitative behavior of the thermal conductivity with respect to variable X_{ES}. Finally, this choice was confirmed to be more suitable since it allows a more universal behavior as shown in Appendix B. Similarly to what has been proposed by Hopp and Gross[10], the $g(\rho)$ function was introduced in order to limit the effect of the corrections to the low density region. In the $g(\rho)$ function, both of the molar density ρ and its critical value ρ_c are calculated by the considered EoS.

It can be observed in Fig. 3 that both of the proposed reductions result in a significant improvement with respect to Fig. 2 where the internal degrees of freedom are not accounted in the definitions of λ_{ref}. Fig. 3 shows that all curves remain closely packed at dense states ($X_{ES} < 0$), except for the case of water. In dilute-gas conditions ($X_{ES} \geq 0$), it is observed that all curves align along a well-defined oblique asymptote when using a reference term $\lambda_{ref}^{Rosenfeld,intDoF}$ (see Fig. 3-A) whereas a roughly-defined horizontal asymptote appears if $\lambda_{ref}^{CE,\ intDoF}$ is used instead (see Fig. 3-B).

Fig. 3-A clearly shows that the selection of $\lambda_{ref}^{Rosenfeld,intDoF}$ as reference term (Eq. 12) makes it possible to achieve a satisfactory description of the thermal conductivity behavior in the liquid, gas and supercritical domains since a monovariable relationship between the reduced thermal conductivity and the X_{ES} variable exists over the entire X_{ES} range. At dense states, although the curves remain closely packed, they exhibit all component-specific behaviors which can be ascribed to the specific interaction and size / shape effects of each chemical specie.

In conclusion, the reference term $\lambda_{ref}^{Rosenfeld,intDoF}$ is well calibrated for defining an entropy scaling relation and thus, is selected definitively for the subsequent parts of this study.

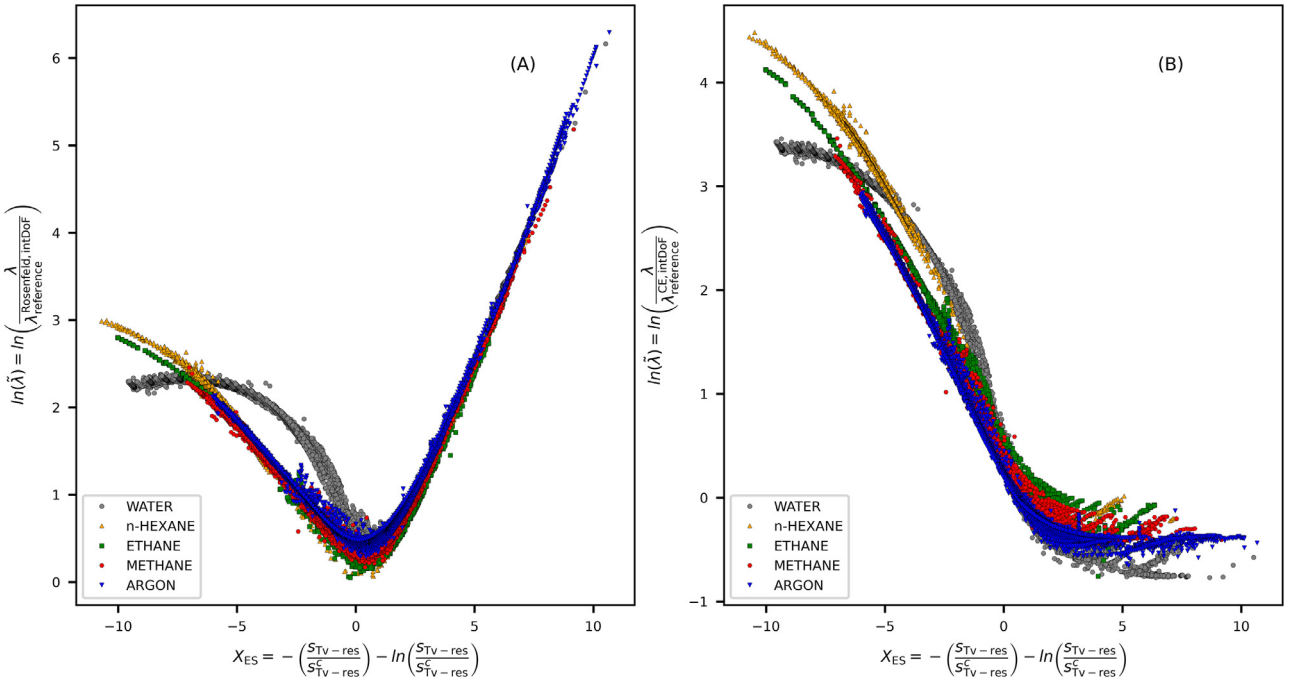

Fig. 3. Plot of the experimental reduced thermal conductivity as a function of the X_{ES} variable using the *I*-PC-SAFT EoS. Subplot (A): using the macroscopic corrected reduction (Eq. (12) and Table 1). Subplot (B): using the microscopic corrected reduction (Eq. (13) and Table 1)

2.4. Functional form for the calculation of the thermal conductivity of real pure fluids

Analogously, to what has been observed for the dynamic viscosity, a quasi-common global minimum is obtained in the $(X_{ES},\ ln(\lambda/\lambda_{ref}^{Rosenfeld,\ intDoF}))$ plane at $X_{ES} \approx 0$ (see Fig. 3-A). As pointed out by Rosenfeld and as mentioned later by Bell et al. [53,54], this minimum reflects a regime changeover between a liquid-like behavior (predominated by intermolecular interactions/forces effects) and a gas-like behavior (predominated by kinetic effects). Following the procedure developed in our study devoted to model fluid viscosity[46] and aimed at describing entropy-scaling curves with a relatively simple fitting function, a decomposition of the reduced thermal conductivity in a logarithm scale into a dense and a gas parts (see Eq. (14)) is carried out.

$$ln\left(\tilde{\lambda}\right)_{calc} = f_{dense}(\tilde{s}_{Tv-res}) \times g_{dense} + f_{gas}(\tilde{s}_{Tv-res}) \times g_{gas} + d \tag{14}$$

In Eq. (14), f_{dense} and f_{gas} are polynomial functions describing the dense-state behaviour (i.e., for $X_{ES} < 0$; note that the term "dense" refers both to subcritical liquid and supercritical fluids) and the dilute-gas behaviors (i.e., for $X_{ES} > 0$); g_{dense} and g_{gas} are damping factors making f_{dense} dominating in the dense region, and conversely, f_{gas} dominating in the gas region; d is a component-specific constant. For the thermal conductivity, the following functional forms are proposed:

$$\begin{cases} f_{dense}(\tilde{s}_{Tv-res}) = \left(a_1 + a_2 X_{ES}^{1/3}\right) X_{ES} \\ g_{dense} = \frac{1}{1+e^{cX_{ES}}} \\ f_{gas}(\tilde{s}_{Tv-res}) = \left(b_1 + b_2 X_{ES}^{1/3}\right) X_{ES} \\ g_{gas} = \frac{1}{1+e^{-cX_{ES}}} \end{cases} \tag{15}$$

where a_1, a_2, b_1, b_2, c and d are six adjustable parameters. Eq. (15) differs from the one used to correlate the viscosity data in our previous work[46] since it uses the X_{ES} variable instead of the Tv-residual entropy in the polynomials. This choice was motivated by the analysis of the experimental data. In short, since the X_{ES} values tend to be similar for different components, the use of this variable facilitates the correlation of the thermal conductivity data when chemical-family specific or universal parameters have to be determined. Indeed, the entropy scaling curves obtained for different molecules with the reference thermal conductivity expression reported in Eq. (12) are closely packed.

Ultimately, the model proposed in this study is defined as:

$$\begin{cases} \ln\left(\frac{\lambda}{\lambda_{ref}^{Rosenfeld,intDoF}}\right)_{calc} = \left[\left(\frac{1}{\frac{a_1+a_2X_{ES}}{1+e^{cX_{ES}}}^{1/3}}\right) + \left(\frac{1}{\frac{b_1+b_2X_{ES}}{1+e^{-cX_{ES}}}^{1/3}}\right)\right] X_{ES} + d \\ \lambda_{ref}^{Rosenfeld,intDoF} = \rho_N^{2/3} k_b \sqrt{\frac{k_b T}{m_0}} \left[1 + \left(\frac{c_v^{real}}{R}\right) e^{-\left(\rho/\rho_c\right)}\right] \\ X_{ES} = -\left(\frac{\tilde{s}_{Tv-res}}{\tilde{s}_{Tv-res}^c}\right) - \ln\left(\frac{\tilde{s}_{Tv-res}}{\tilde{s}_{Tv-res}^c}\right) \text{for the I} - \text{PC} - \text{SAFT EoS} \\ X_{ES} = -\left(\frac{\tilde{s}_{Tv-res}}{\tilde{s}_{Tv-res}^c}\right) - \ln\left\{\left(\frac{\tilde{s}_{Tv-res}}{\tilde{s}_{Tv-res}^c}\right)\left[1+\alpha\left(\frac{T-T_c}{T_c}\right)^3\right]\right\} \text{for the tc} - \text{PR EoS} \end{cases} \tag{16}$$

As previously stated, in Eq. (16), the α coefficient is an optional component-specific parameter to be used with the *tc*-PR EoS only, for light components only. It enables to improve thermal conductivity predictions for reduced temperatures in the range: $4 < T_r < 8$.

Fig. 4 shows characteristic vapor–liquid saturation curves as well as series of liquid, gas and supercritical branches of various isotherms for the case of methane modelled with the *I*-PC-SAFT EoS [21]. These curves are represented in the $(P_r,\ Y_{ES},\ X_{ES})$ space (see Fig. 4-A), where $P_r = P/P_c$ denotes the reduced pressure and $Y_{ES} = \ln(\tilde{\lambda})$ is the natural logarithm of the reduced thermal conductivity, in the $(P_r,\ X_{ES})$ plane (see Fig. 4-B), and in the (Y_{ES}, X_{ES}) plane (see Fig. 4-C). As shown in Fig. 4-C, Eq. (16) achieves an excellent correlation of the reduced thermal conductivity along all fluid conditions, when the parameters a_1, a_2, b_1, b_2, c and d are fitted to experimental data for a given chemical component. More-

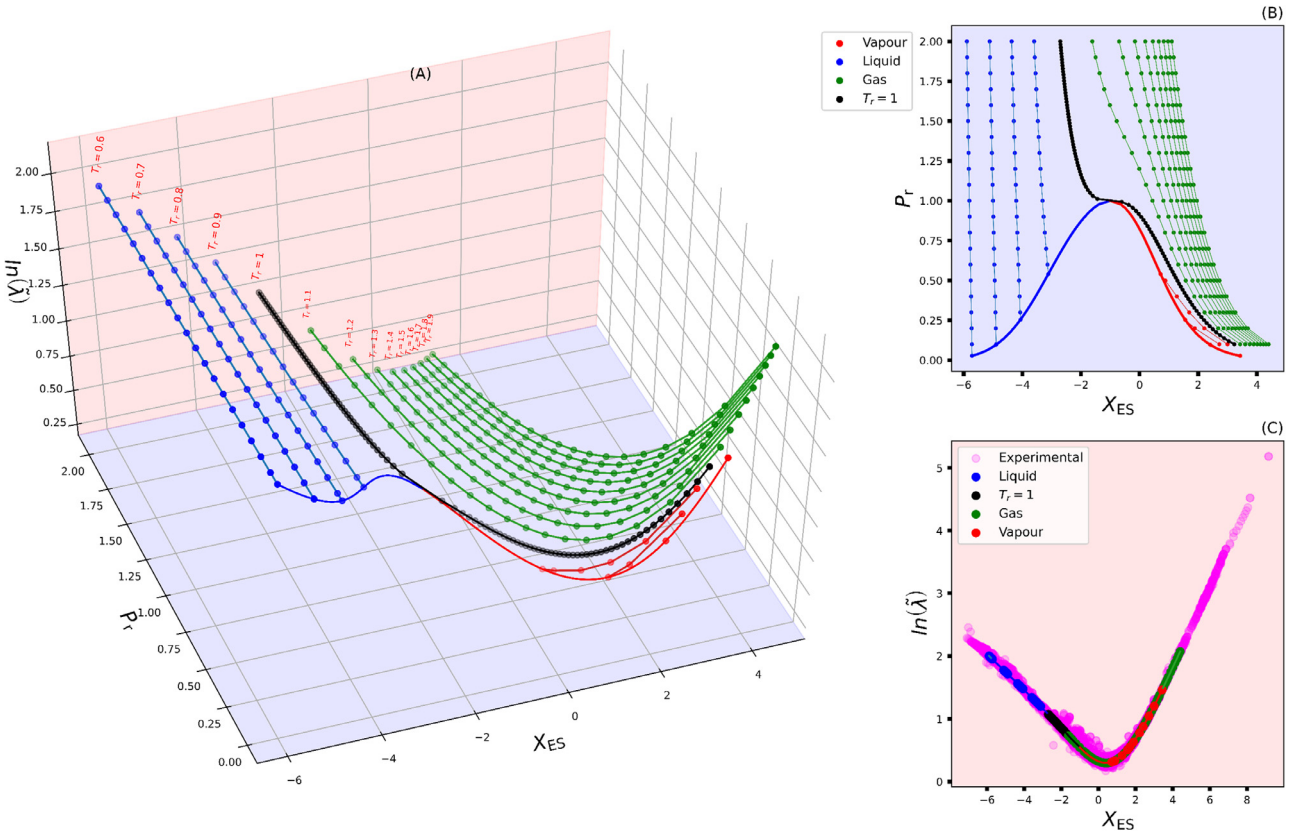

Fig. 4. Graphical illustration of the entropy scaling formulation proposed in this paper using the *I*-PC-SAFT EoS through the representation of isotherms and saturation curves of pure methane in 3 different diagrams. Reduced temperatures of isotherms range from $T_r = 0.6$ to 1.9 while reduced pressures span from $P_r = 0.1$ to 2. Subplot (A): representation in the (P_r, $ln(\tilde{\lambda})$, X_{ES}) space as calculated with the *I*-PC-SAFT EoS, Subplot (B): representation in the (P_r, X_{ES}) plane as calculated with the *I*-PC-SAFT EoS. Subplot (C): representation in the ($ln(\tilde{\lambda})$, X_{ES}) plane of the same isotherms and saturation curves and comparison with the experimental data.

over, the combination of the X_{ES} variable and the $\lambda_{ref}^{Rosenfeld,intDoF}$ reference thermal conductivity ensures that the liquid and gas-like states align along a single curve in the ($\ln(\tilde{\lambda})$, X_{ES}) plane. According to Eq. (10), the critical point is located at $X_{ES} = -1$.

3. Results & discussion

A large database of experimental thermal conductivities was extracted from the commercial Dortmund Data Bank [45] in order to determine 3 sets of model parameters: (i) component-specific, (ii) chemical-family specific (i.e., common to all compounds of a given chemical family) and (iii) universal (i.e., usable for any component without restriction) for each of the two proposed models obtained by combining Eq. (16) with either the *tc*-PR or the *I*-PC-SAFT EoS. The database encompasses liquid, gas and supercritical data for 119 chemical components belonging to 11 different chemical families. Around 90,000 experimental data points were included; their temperatures range from 25 to 3600 K; the pressures range from 10^{-4} to 10^{3} MPa and thermal conductivities span from 0.004 to 0.78 $W \cdot m^{-1} \cdot K^{-1}$.

Some experimental data points were removed from the database after application of the following filters:

- Data associated with pressures out of the range [10^{-3} MPa; 10^{2} MPa] were considered as potentially inaccurate and disregarded,
- The present model does not account for the *critical enhancement of the thermal conductivity*, so that data in the close critical region ($0.95 < T_r < 1.05$ and $0.95 < P_r < 1.05$) were also removed. In addition, data such that $T_r > 8$ were removed when the *tc*-PR EoS was used because they are outside the domain of validity of Eq. (11).

To eliminate out-of-chart data, the absolute deviation $Y^i = |Y^i_{calc} - Y^i_{exp}|$, where $Y = \ln\tilde{\lambda}$, was calculated for each data point of a given component and compared to the corresponding average deviation $\overline{\Delta Y}$ estimated over all the data points for the species under consideration. It was decided to disregard data such that: $\Delta Y^i > \overline{\Delta Y} + 3\sigma$ (where σ denotes the standard deviation). For clarity, it is recalled that ΔY^i is calculated as: $\Delta Y^i = |\ln(\frac{\lambda_{calc,i}}{\lambda_{ref}}) - \ln(\frac{\lambda_{exp,i}}{\lambda_{ref}})|$ where $\lambda_{ref} = \rho_N^{\frac{2}{3}} k_b \sqrt{m_0 T / k_b} [1 + (\frac{c_v^{real}}{R}) e^{-(\rho/\rho_c)}]$ is calculated by the EoS.

To determine the values of the 6 parameters defined in Eq. (16) (a_1, a_2, b_1, b_2, c and d) as well as the α coefficient when necessary (i.e., for light molecules modelled with the *tc*-PR EoS), the following objective function F^{λ}_{obj} was minimized with respect to the 6 (or 7, with α) coefficients:

$$F^{\lambda}_{obj} = \frac{100}{Nb_{data}} \sum_{i=1}^{Nb_{data}} 0.5 \frac{|\lambda_{calc,i} - \lambda_{exp,i}|}{\lambda_{exp,i}} + 0.5 \frac{|Y_{calc,i} - Y_{exp,i}|}{Y_{exp,i}} \quad (17)$$

where Nb_{data} denotes the total number of the considered experimental data and $Y_{exp,i}$ and $Y_{calc,i}$ are respectively, the logarithm of the experimental and the calculated values (according to Eq. (16)) of the reduced thermal conductivity at the temperature and pressure of the experimental data point i, $\lambda_{exp,i}$ and $\lambda_{calc,i}$ are respectively the equivalent experimental and calculated values of the thermal conductivity. Eq. (17) averages relative deviations on the thermal conductivity (λ) but also on $Y_{ES} = \ln(\tilde{\lambda})$. MAPE on λ is included in Eq. (17) since our primary objective is to model accu-

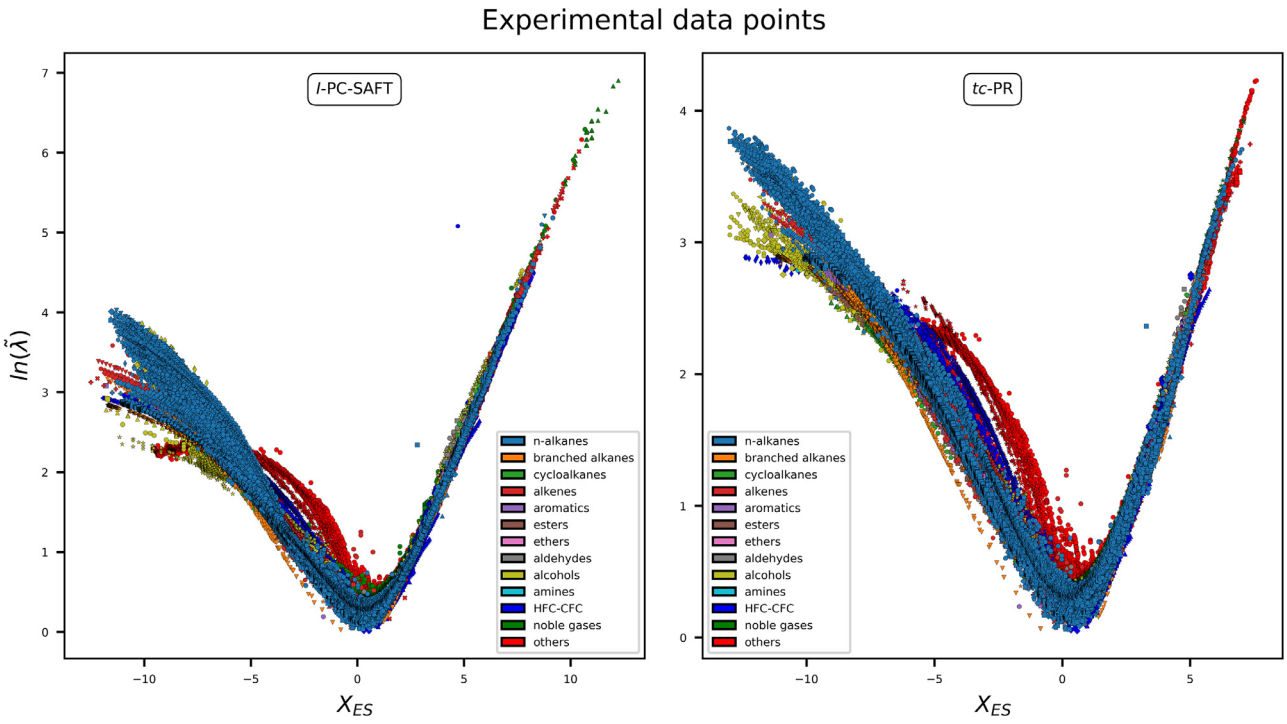

Fig. 5. Overview of all the experimental data in the $(\ln\tilde{\lambda},\ X_{ES})$ plane. The thermodynamic properties involved in the calculation were estimated with the *I*-PC-SAFT EoS in the left subplot and with *tc*-PR EoS in the right subplot. Each color corresponds to a chemical family and each symbol corresponds to a given chemical specie.

rately the thermal conductivity. It was decided to add MAPE on Y_{ES} to help the convergence of the minimization procedure. Since the thermal conductivities undergo an evolution of several orders of magnitude from dense liquids to dilute gases, the consideration of the logarithm of the reduced coefficient which evolves under values having the same order of magnitude ensures that errors on both the dilute state and the dense state have a similar impact on the optimization procedure.

The minimization of Eq. (17) was performed using the Broyden-Fletcher-Goldfarb-Shanno (BFGS) algorithm, a quasi-Newton optimization method. To ensure the robustness of the optimized parameter sets by avoiding dependence on initial estimates and convergence to local minima, multiple initialization sets were systematically generated using a random process for each compound.

Among all the parameter sets returned by the routine, the optimal one was identified as follows:

- At least half of the initial guesses led to the same optimal parameter set,
- This parameter set was associated with the lowest objective function value and a nearly-zero gradient norm.

Fig. 5, gathers all the obtained entropy scaling curves, for each of the EoS considered here, for all chemical components, in the $(\ln\tilde{\lambda},\ X_{ES})$ plane. A detailed description of experimental data is provided in sections 1.1 and 2.1 of the supporting information file. As pointed out above, V-shapes curves are obtained for the thermal conductivity with a quasi-common minimum in the vicinity of $X_{ES} \approx 0$ and a quasi-universal linear behaviour at low densities. In addition, it is also noticeable that entropy scaling curves exhibit a concave profile at high density.

3.1. Component-specific parameters

The component-specific parameters were obtained by minimizing Eq. (17) against the experimental data of each chemical component. Important details regarding the strategy used to fit model parameters, depending on the availability of experimental data, are reported in Table 2 of appendix C. Figs. 6 to 9 show the results obtained by combining the *I*-PC-SAFT and the *tc*-PR EoS with component specific parameter sets (a_1, a_2, b_1, b_2, c and d). These parameter sets are provided for all the considered chemical species in sections 1.2 and 2.2 of the supporting information file. As observable in Figs. 6 to 9, the functional form proposed in Eq. (16) is flexible enough to ensure a very accurate description of the thermal conductivity over the whole fluid domain, regardless of the considered EoS and regardless of the chemical nature of species (from non-associating and non-polar compounds like n-alkanes which reports experimental uncertainties between 5 to 10% to more complex molecules like alcohols or water reporting from 5 to 25% of uncertainty in the experimental measures). As previously observed to predict vapor-liquid equilibrium properties[50], the 2 considered EoSs that do not contain an association term lead to very similar results. The detailed MAPEs for several chemical families (calculated by averaging the MAPEs of all the compounds present in a given chemical family) are shown in Fig. 10. It can be seen that nearly all the deviations are below 3%, regardless of the considered chemical family. For the studied species, the deviations obtained by the presented models are within or below the experimental uncertainties and thus, the models allow accurate prediction for thermal conductivity. These results contrast with the findings of Dyre, who pointed out that the entropy scaling might not work in most systems with strong directional bonds like hydrogen-bonded or covalently bonded systems.

3.2. Chemical-family specific parameters

In order to estimate the thermal conductivity of a particular species for which a limited amount or no experimental data is available but that belongs univocally to a chemical family considered in this work (e.g., paraffins, alcohols ...), for which enough data were available to estimate model parameters, it was decided

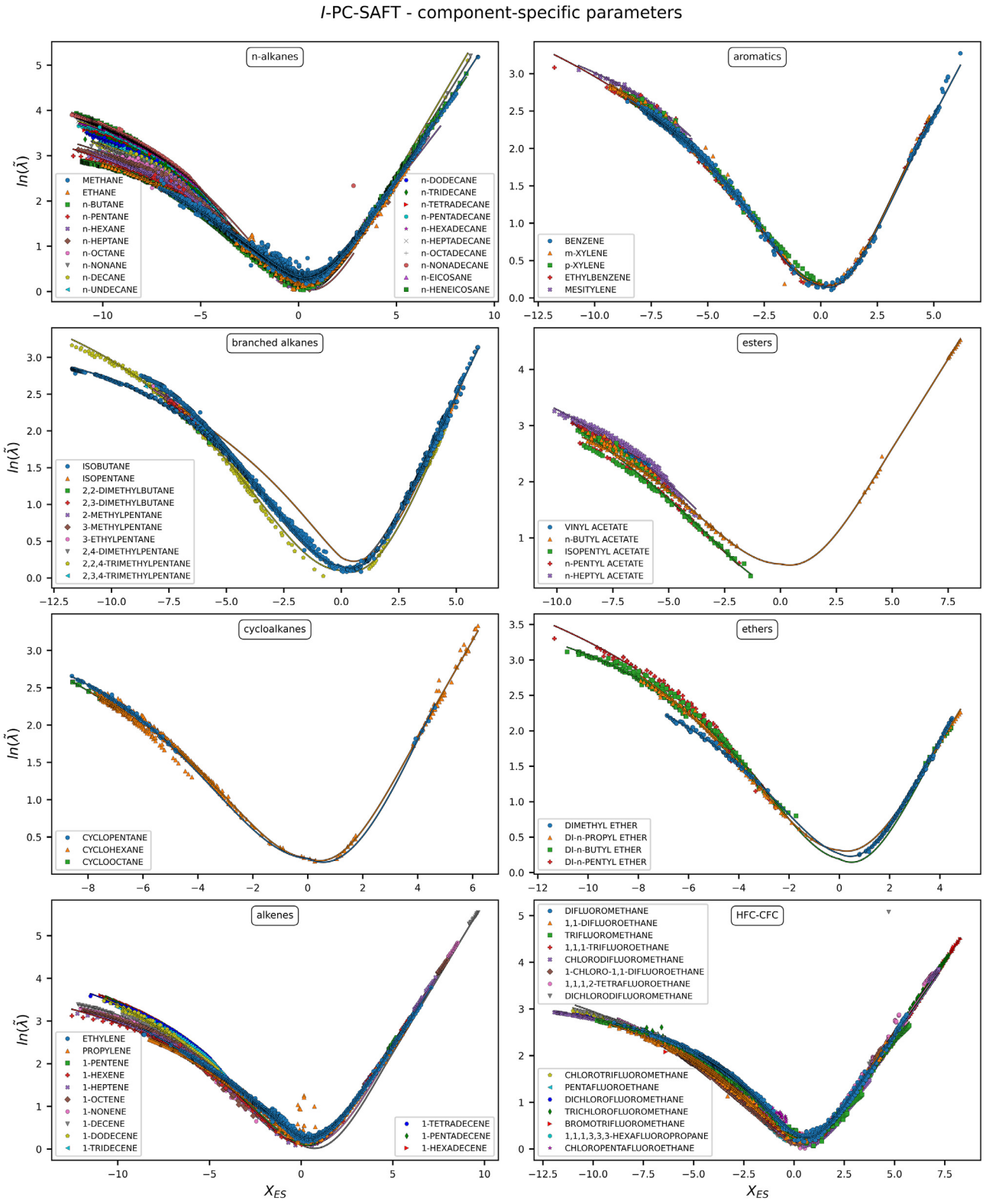

Fig. 6. Results of the combination of the component-specific parameters with the *I*-PC-SAFT EoS for modelling the thermal conductivity of n-alkanes, branched alkanes, cycloalkanes, alkenes, aromatics, esters, ethers and HFC-CFCs. Symbols represent the experimental data points; Solid lines represent the calculated values.

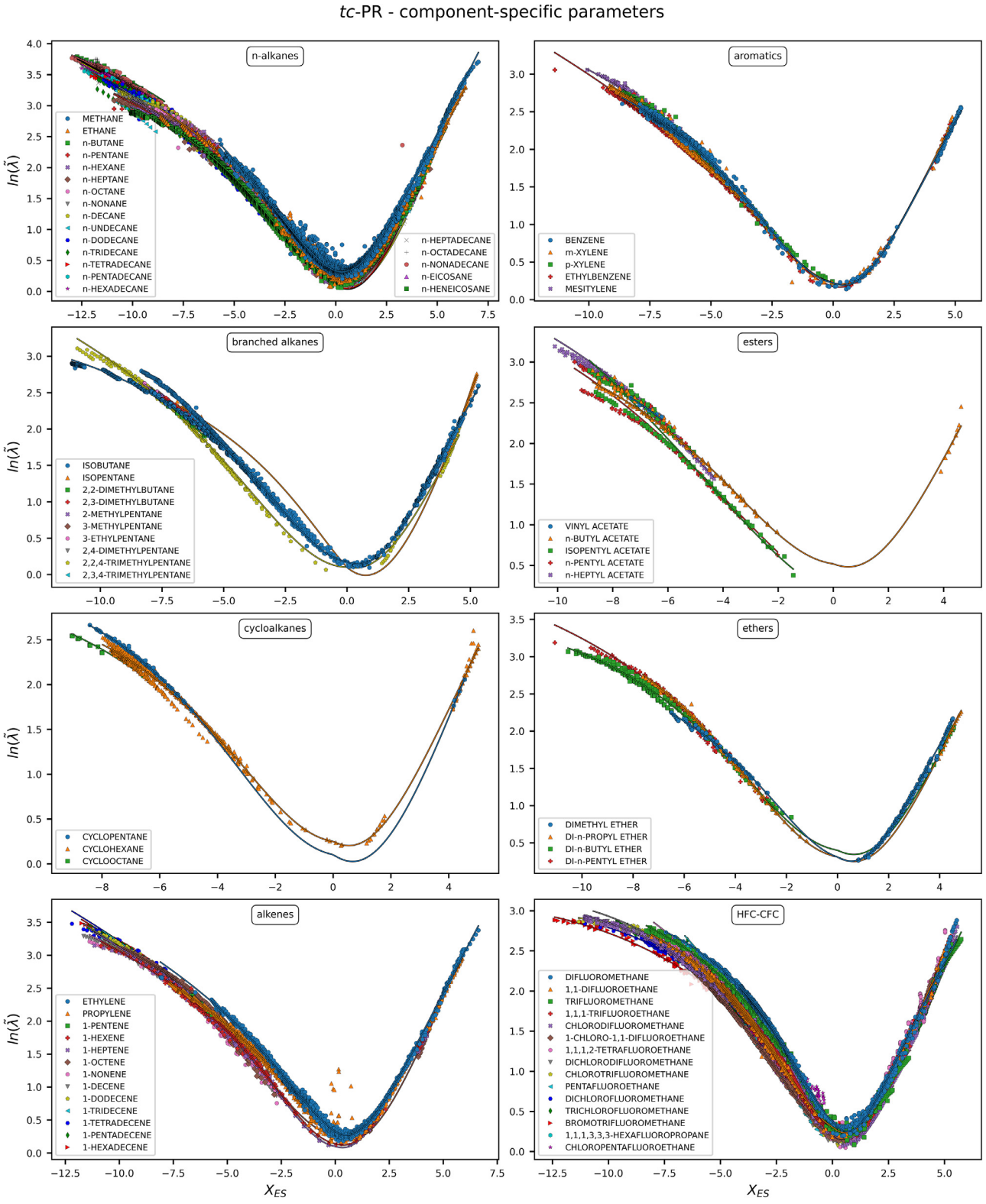

Fig. 7. Results of the combination of the component-specific parameters with the *tc*-PR EoS for modelling the thermal conductivity of n-alkanes, branched alkanes, cycloalkanes, alkenes, aromatics, esters, ethers and HFC-CFCs. Symbols represent the experimental data points; Solid lines represent the calculated values.

to propose chemical-family specific parameters. 10 chemical families including alcohols and amines were selected. Figs. 11 and 12 show the obtained results for the paraffins (n-alkanes and branched alkanes) and the HFC-CFCs families with both the *I*-PC-SAFT and the *tc*-PR based models.

As stated above, parameters (a_1, a_2, b_1, b_2, c and d) were fitted to all the experimental data related to all the compounds of a given chemical family. A detailed analysis of such figures makes it possible to draw the following conclusion: regarding the dense states, it has to be noted that although the same reduction of the

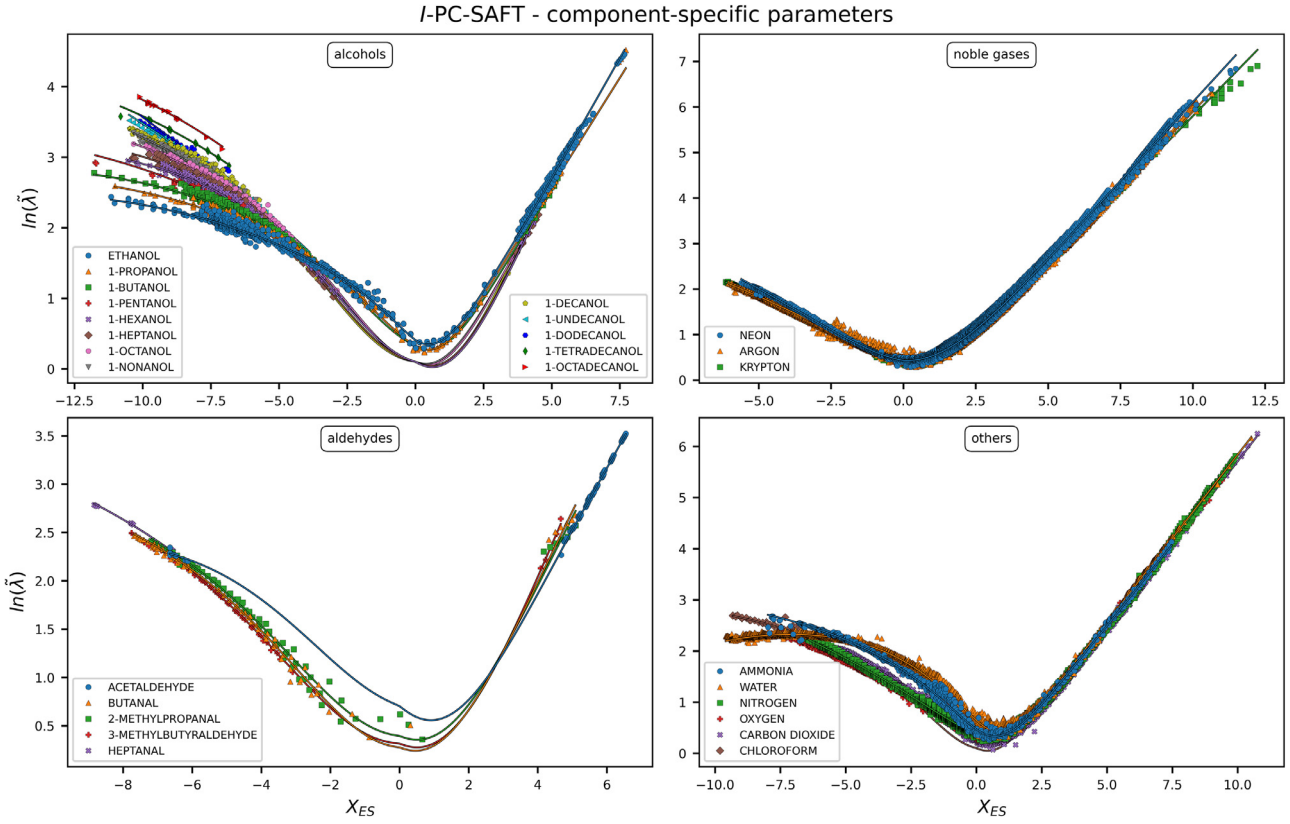

Fig. 8. Results of the combination of the component-specific parameters with the *I*-PC-SAFT EoS for modelling the thermal conductivity of alcohols, noble gases, aldehydes and other chemical species. Symbols represent the experimental data points; Solid lines represent the calculated values.

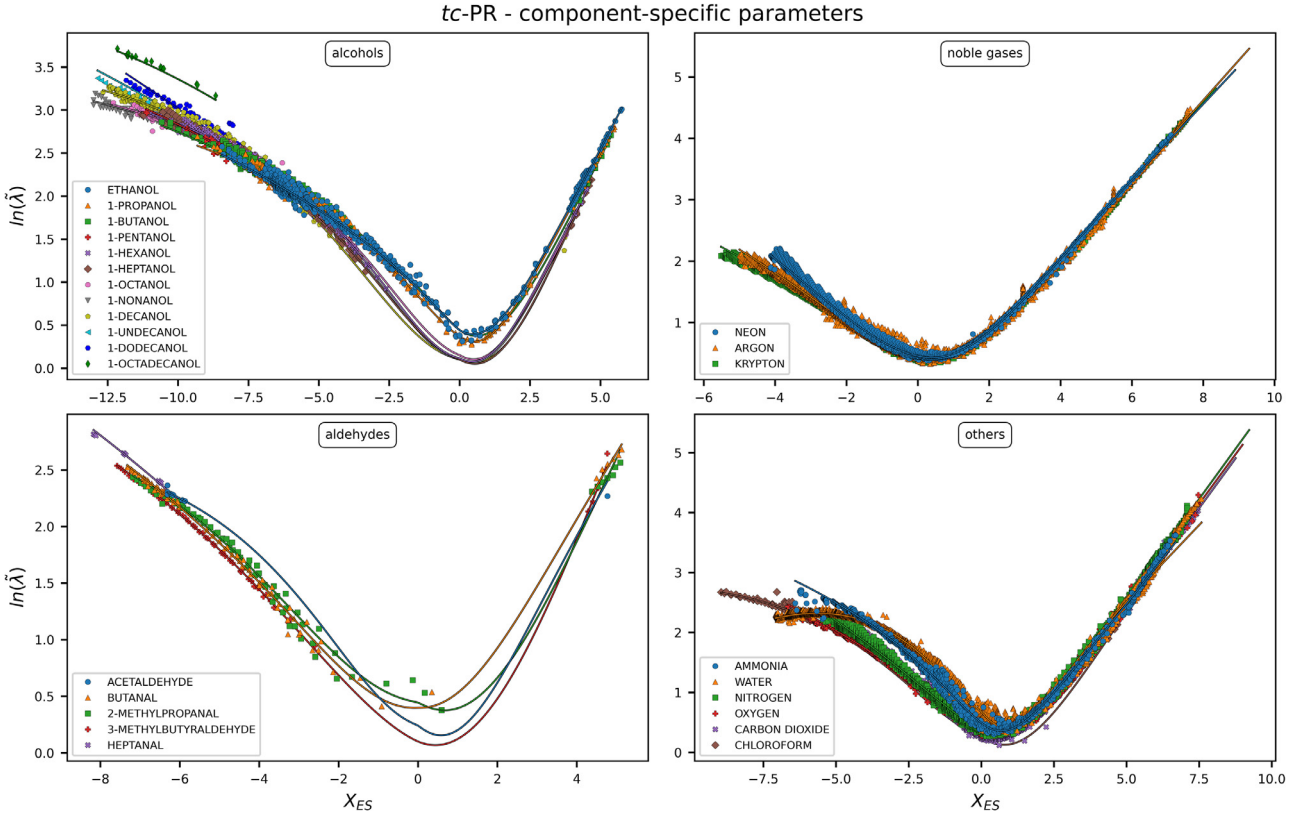

Fig. 9. Results of the combination of the component-specific parameters with the *tc*-PR EoS for modelling the thermal conductivity of alcohols, noble gases, aldehydes and other chemical species. Symbols represent the experimental data points; Solid lines represent the calculated values.

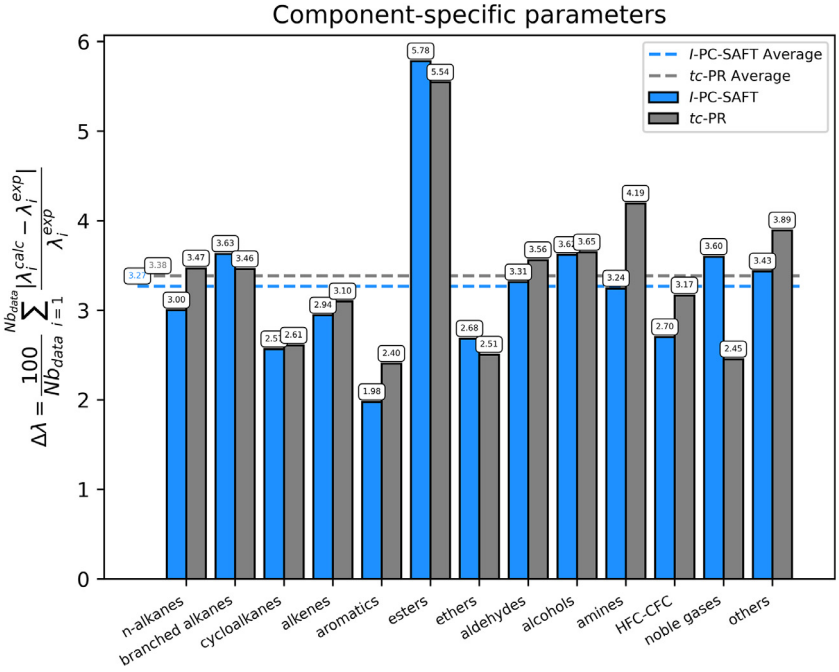

Fig. 10. Summary of MAPEs obtained with the *I*-PC-SAFT and the *tc*-PR EoS in combination with the component-specific parameters

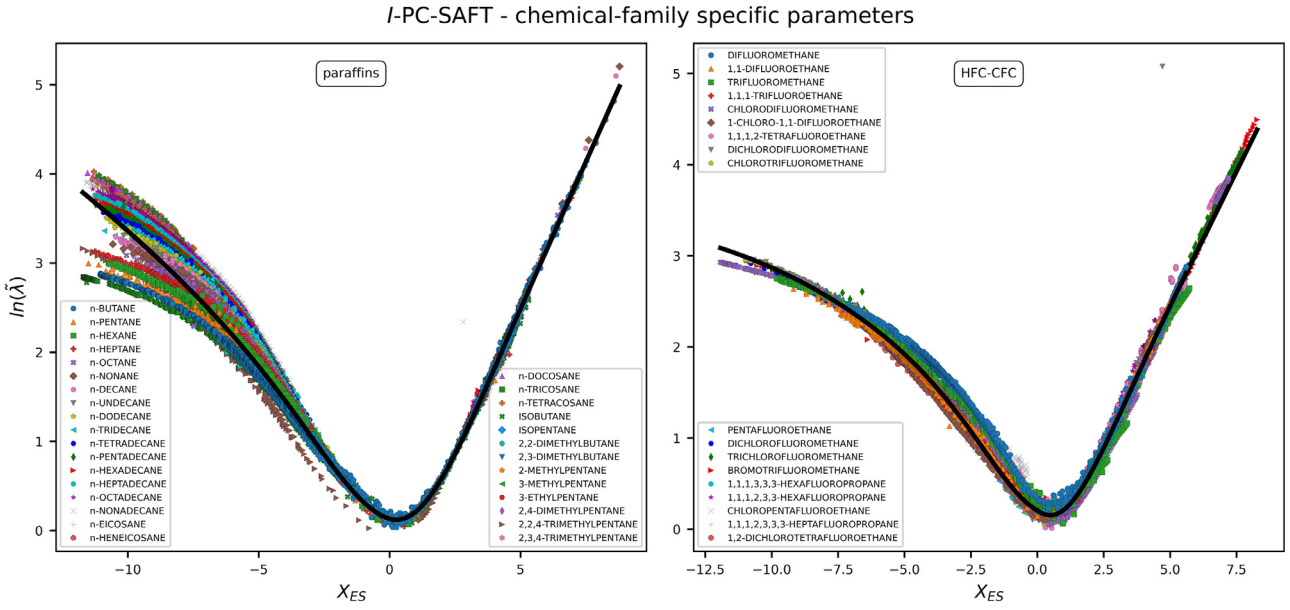

Fig. 11. Results of the combination of the chemical-family specific parameters with the *I*-PC-SAFT EoS for modelling the thermal conductivity of paraffins and HFC-CFCs. Symbols represent the experimental data points; Solid lines represent the calculated values.

thermal conductivity is applied to both EoS, a different behavior of the entropy scaling curves (i.e., more or less pronounced curve slopes, different ordering …) is observed between both EoS predictions. This effect is the consequence of the Tv-residual entropy values returned by each EoS and is revealed by the comparison between component-specific curves of a same homologous series that were calculated with the two considered EoS. For illustration, let us consider the particular cases of the n-alkane and alcohol molecules. For these 2 chemical families, packed curves were obtained with the *tc*-PR model (see Figs. 7 and 9) whereas distinct component-specific curves can be observed at high absolute values of $\tilde{s}_{\mathrm{Tv-res}}$ when the *I*-PC-SAFT EoS is used (see Figs. 6 and 8). This particular *I*-PC-SAFT behavior has an immediate negative impact on the ability of a chemical-family specific set of parameters to describe the thermal conductivity of the complete family. This impact is depicted in Fig. 13 where the thermal conductivities of paraffins (which encompass n-alkanes and branched-alkanes) and alcohols respectively exhibit a MAPE of 15.6% and 17 % for the *I*-PC-SAFT model while these values are respectively 5.9 and 5.5 % with the *tc*-PR model. For all the other chemical families such as HFC-CFCs, the predicted thermal conductivities agree with the experimental data (see Figs. 11 and 12) and the MAPEs (see Fig. 13) remain within the experimental uncertainties for both EoS. Although not more accurate than the *I*-PC-SAFT EoS, the *tc*-PR EoS seems to be better suited to defining chemical-family specific parameters.

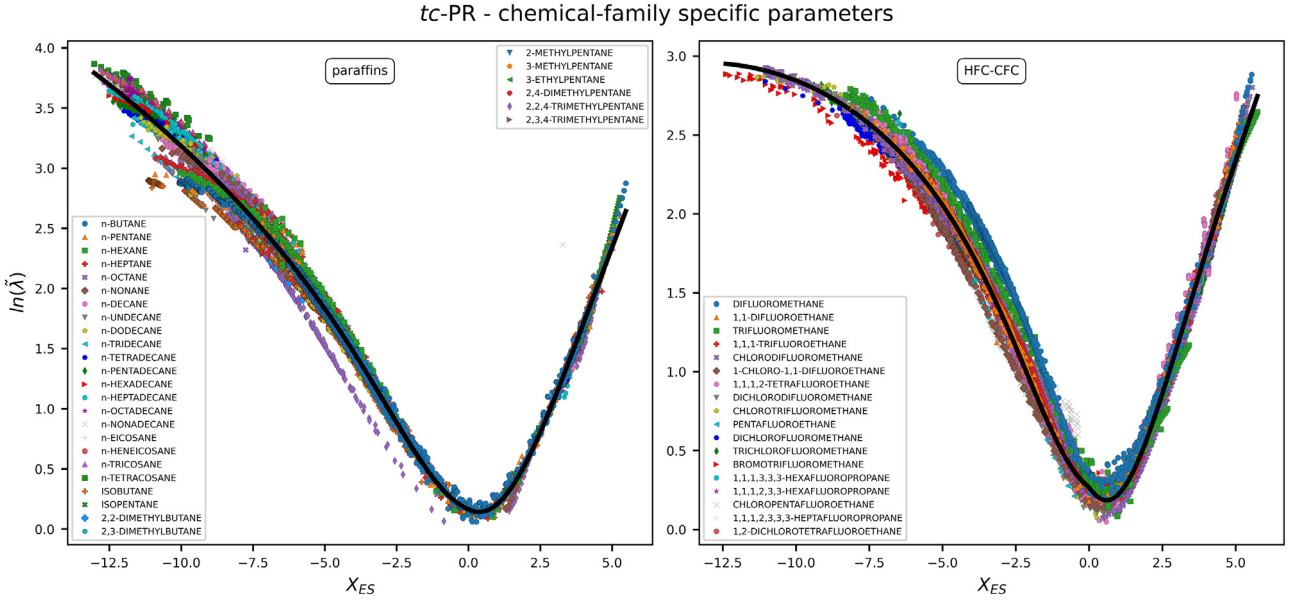

Fig. 12. Results of the combination of the chemical-family specific parameters with the *tc*-PR EoS for modelling the thermal conductivity of paraffins and HFC-CFCs. Symbols represent the experimental data points; Solid lines represent the calculated values.

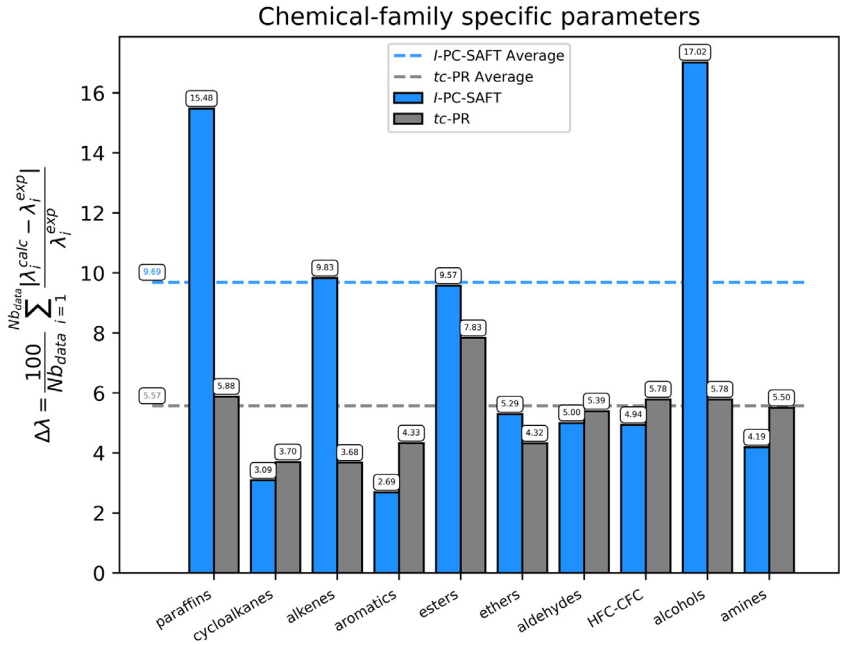

Fig. 13. Summary of MAPEs obtained with the *I*-PC-SAFT and the *tc*-PR EoS in combination with the chemical-family specific parameters

3.3. Universal parameters

As a last resort for chemical species that do not belong to one of the ten chemical families previously defined and for which a limited number of experimental data is available, it was decided to fit universal parameters against all the available experimental data of all the compounds as a whole. Some components with a specific behavior like water or noble gases which possess a small number of internal degrees of freedom were disregarded in order not to bias the estimation of these parameters. Such universal parameter sets (one set per EoS) aim to afford a reasonable estimation of the thermal conductivity of a pure fluid knowing as sole input data: its critical temperature T_c, critical pressure P_c, acentric factor and the volume translation c for the *I*-PC-SAFT model or T_c, P_c, c and the three component-specific alpha-function parameters (L, M, N) for the *tc*-PR model. These parameters make it possible:

- to qualitatively reproduce the temperature and pressure dependence of the pure fluid thermal conductivities.
- to predict with a reasonable accuracy the thermal conductivities of any chemical species as reported in Fig. 15 where the overall MAPEs are respectively 11.2% and 9.2% for the *I*-PC-SAFT and the *tc*-PR models (more detailed information is provided in section 1.4 and 2.4 of the supporting information file),
- to get a continuous representation of thermal conductivity over the three fluid regions (liquid, gas and supercritical) for any given component, as shown in Fig. 14

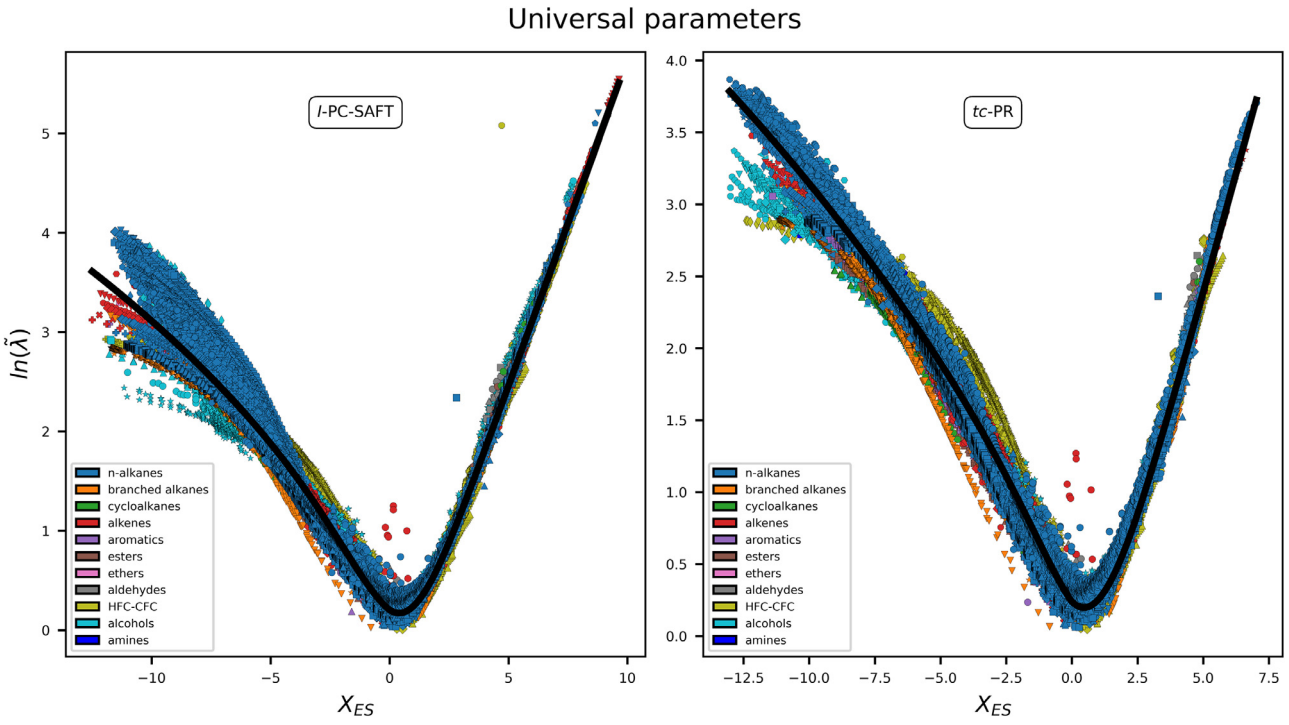

Fig. 14. Results of the combination of the universal parameters with the *l*-PC-SAFT and the *tc*-PR EoS for modelling the thermal conductivity. Each color corresponds to a chemical family and each symbol correspond to a given chemical specie; Solid lines represent the calculated values.

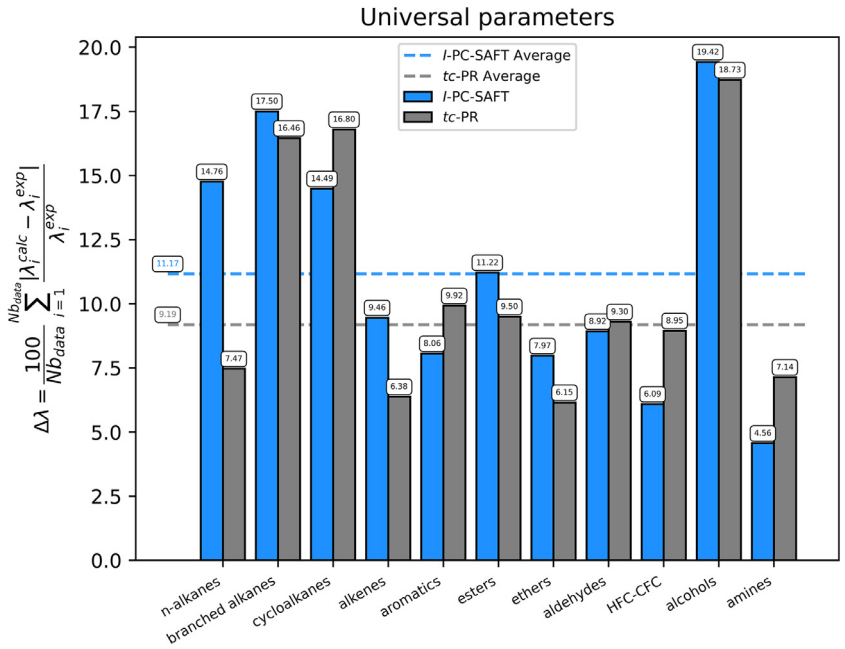

Fig. 15. Summary of MAPEs obtained with the *l*-PC-SAFT and the *tc*-PR EoS in combination with the universal parameters.

4. Conclusion

In this study, a successful combination between a Tv-residual entropy dependent function, which was previously derived for the dynamic viscosity, and a corrected reference thermal conductivity are proposed for the calculation of the thermal conductivities of pure fluids through the entropy scaling concept. Two equations of states (*I*-PC-SAFT and *tc*-PR) were used to predict the residual entropy and other needed properties (density, residual isochoric heat capacity) thus yielding to the definition of two models. The approach was validated against a large experimental database and made it possible to conclude that:

- using component-dependent parameters, the thermal conductivities of pure fluids could be accurately correlated with an average deviation of only 3% which is really promising.
- The thermal conductivities can be estimated regardless of the fluid state: liquid, gas and supercritical. The critical region was excluded, however, since the critical enhancement of thermal conductivities was not considered in this study.
- The proposed model follows the general entropy-scaling relation for thermal conductivity: $\lambda_{\text{real}} = \lambda_{\text{reference}} \times f(s_{\text{Tv-residual}})$. The quantities: $\lambda_{\text{reference}}$ and $f(s_{\text{Tv-residual}})$ are defined by Eq. (16) and can be straightforwardly estimated from an EoS. In this paper, both the *I*-PC-SAFT and *tc*-PR EoS were used.
- To overcome the lack or unavailability of experimental data of some chemical species, chemical-family specific and universal versions of model parameter sets were fitted in addition to the component-specific ones. The overall MAPEs obtained with the *I*-PC-SAFT and the *tc*-PR EoS are respectively 9.7% and 5.6 % when the parameters are chosen chemical-family specific and 11.2% and 9.2% when they are considered as universal which is accurate enough for many industrial applications.

As this approach involves only macroscopic thermodynamic quantities, accessible via an equation of state, it is believed that it can be straightforwardly implemented.

In a future work, the extension of the proposed model to mixtures will be investigated.

5. Notations and Symbols

a Helmholtz energy (J)
c_v Specific heat capacity at constant volume ($J \cdot mol^{-1} \cdot K^{-1}$)
k_b Boltzmann constant ($J \cdot K^{-1}$)
N_a Avogadro's number (mol^{-1})
m_0 Molecular mass (kg)
m Chain length (molecular parameter used when the fluid is modelled as a chain of spheres)
P Pressure (Pa)
P_c Critical pressure (Pa)
P_r Reduced pressure P/P_c
T Temperature (K)
T_c Critical temperature (K)
T_r Reduced temperature T/T_c
v Molar volume ($m^3 \cdot mol^{-1}$)
s Molar entropy ($J \cdot mol^{-1} \cdot K^{-1}$)
s^c Critical value of the molar entropy ($J \cdot mol^{-1} \cdot K^{-1}$)
$\tilde{s}$ Reduced (dimensionless) molar entropy (s/R)
$\tilde{s}^c$ Critical value of the reduced molar entropy
X_{ES} X-coordinate used for the application of our entropy-scaling (ES) approach $X_{ES} = -(\frac{\tilde{s}_{Tv-res}}{\tilde{s}^c_{Tv-res}}) - \ln(\frac{\tilde{s}_{Tv-res}}{\tilde{s}^c_{Tv-res}})$
X^c_{ES} Critical value of X_{ES}
$X^{corrected}_{ES}$ $=X_{ES}$ expression including a *tc*-PR-specific correction for extending its range of applicability ($T_r > 4$).
Y_{ES} Y-coordinate used for the application of the proposed entropy-scaling (ES) approach ($Y_{ES} = \ln(\tilde{\lambda})$)
ε/k_b Molecular attraction parameter, used in molecular models and SAFT-type EoS
λ Thermal conductivity ($W \cdot m^{-1} \cdot K^{-1}$)
λ_0 Thermal conductivity of a dilute gas ($W \cdot m^{-1} \cdot K^{-1}$)
$\Delta\lambda_c$ Thermal conductivity contribution due to the critical enhancement in the vicinity of the critical point ($W \cdot m^{-1} \cdot K^{-1}$)
$\Delta\lambda$ Residual thermal conductivity contribution ($W \cdot m^{-1} \cdot K^{-1}$)
$\lambda_{\text{reference}}$ Reference thermal conductivity (used for thermal conductivity scaling) ($W \cdot m^{-1} \cdot K^{-1}$)
$\tilde{\lambda}$ Reduced thermal conductivity defined as $\frac{\lambda_{\text{real}}}{\lambda_{\text{reference}}}$
η Dynamic viscosity (Pa·s)
D_{self} Self-diffusion coefficient ($m^2 \cdot s^{-1}$)
ρ Molar density ($mol \cdot m^{-3}$)
ρ_N Molecular density (number of molecules per m^{-3})
σ Segment diameter (at 0 K) or collision diameter (m)
$\Omega^{(l,s)*}$ Lennard-Jones collision integral

5.1. Indices

Tv – res Residual property in (T, v) conditions (difference between the real-state property and the perfect-gas property at fixed T and v)
real Real-fluid state
tr Contribution due to molecular translations
int Contribution due to internal degrees of freedom
intDoF Internal degrees of freedom

Declaration of Competing Interest

The authors declare that they have no known competing financial interests or personal relationships that could have appeared to influence the work reported in this paper.

CRediT authorship contribution statement

Aghilas Dehlouz: Conceptualization, Writing – original draft, Writing – review & editing, Software. **Jean-Noël Jaubert:** Conceptualization, Writing – original draft, Writing – review & editing. **Guillaume Galliero:** Validation. **Marc Bonnissel:** Validation, Resources. **Romain Privat:** Conceptualization, Writing – original draft, Writing – review & editing.

Supplementary materials

Supplementary material associated with this article can be found, in the online version, at doi:10.1016/j.ijheatmasstransfer.2022.123286.

Appendix

Appendix A. Graphical illustration of the effect of the tc-PR specific patch to correlate the thermal conductivity at high temperatures

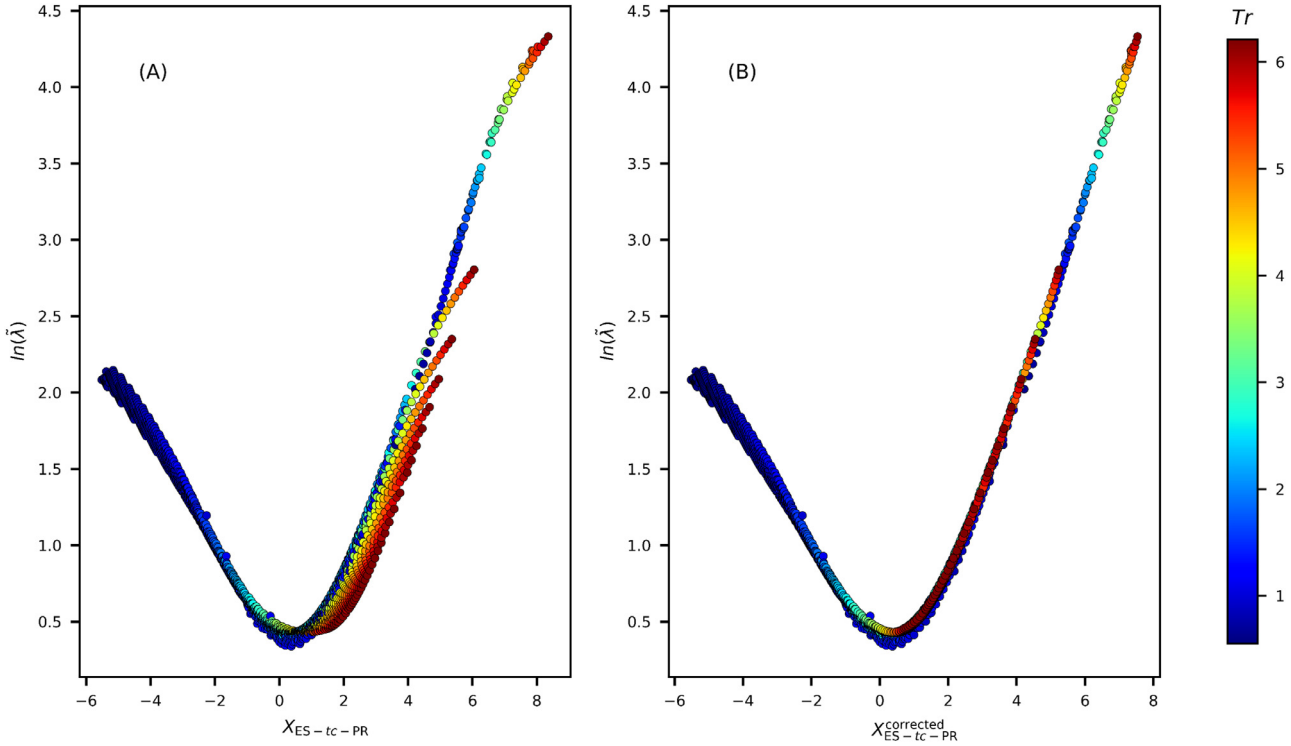

Fig. 16. Comparison between the non-corrected version of the X_{ES} variable (Subplot A) defined in Eq. (10) and the corrected version (Subplot B) given in Eq. (11) in combination with the *tc*-PR Eos for the case of Krypton

Appendix B. Comparison between the use of the total specific heat capacity at constant volume and its contribution due to vibrational and rotational internal degrees of freedom in the definition of the reference thermal conductivity

Fig. 17 reports a comparison between the entropy scaling curves obtained by considering c_v^{real} in subplot A and in subplot B, $c_{v,int} = c_v^{real} - c_{v,tr}$ (with $c_{v,tr} = 3R/2$) for the definition of the reference thermal conductivity reported in Eq. (12) and Table 1. As pointed out in section II.C, this figure shows that a more universal behavior is achieved by considering the total specific heat capacity c_v^{real} of the real fluid while the qualitative aspect of the curves is only slightly influenced by this choice. In subplot B, it can be observed that simple molecules like Argon for which $c_v^{real} \to c_{v,tr} = 3R/2$ and thus $c_{v,int} \to 0$, exhibit higher reduced thermal conductivities (y-coordinates) at low densities ($X_{ES} \geq 0$) than other molecules, such

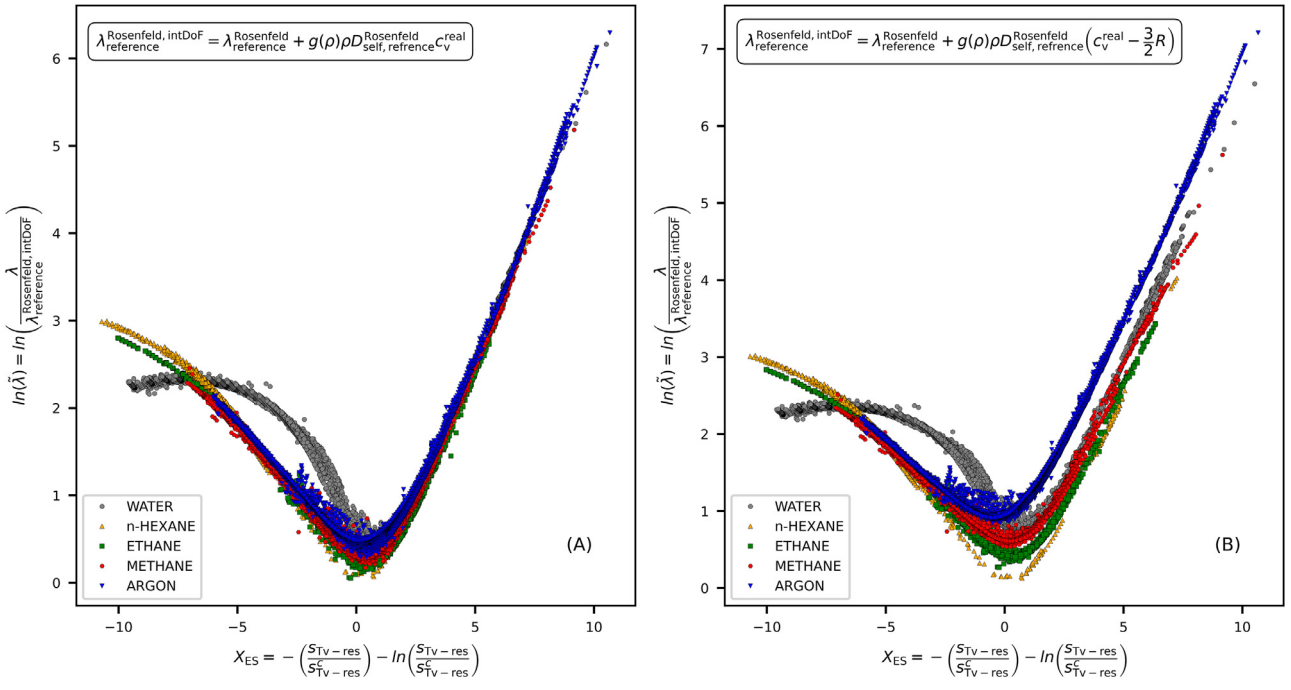

Fig. 17. Comparison between consideration of the total specific heat capacity at constant volume (Subplot A) and its contribution due to vibrational and rotational degrees of freedom (Subplot B) in the definition of the reference thermal conductivity reported in Eq. (12) and Table 1. The thermodynamic quantities are generated by the *I*-PC-SAFT EoS.

Table 2
Strategy for fitting component-specific parameters depending on the availability of experimental data.

Number of experimental data points at dense state	Number of experimental data points at dilute state	Values of the $\boldsymbol{a}_1$ and $\boldsymbol{a}_2$ parameters	Values of the $\boldsymbol{b}_1$, $\boldsymbol{b}_2$, $\boldsymbol{c}$ and $\boldsymbol{d}$ parameters
$\boldsymbol{Nb_{data}}(\boldsymbol{X_{ES}} < 0) \geq 5$	$Nb_{data}(X_{ES} \geq 0) > 3$	Specific to the chemical component	Specific to the chemical component
	$Nb_{data}(X_{ES} \geq 0) < 3$		Fixed to the chemical-family values (fixed to the universal values when non-available)
$\boldsymbol{Nb_{data}}(\boldsymbol{X_{ES}} < 0) < 5$	Component-specific parameters not ascertained.		

as n-hexane, for which $c_{v,int} > 0$. Therefore, considering $c_{v,int}$ rather than c_v^{real} will induce an up-shifting of entropy scaling curves for molecules with negligible degrees of freedom like monoatomic and simple gases.

Appendix C. Optimisation strategy for model parameters

In order to ensure a safe and transparent estimation of model parameters, especially at low density states where a quasi-universal behavior is observed (see Fig. 5), the optimization procedure was defined as follows:

- Universal parameters were obtained considering the many components reported in Figs. 14 and 15.
- Chemical-family specific parameters were optimized considering each family as a whole. b_1, b_2, c and d parameters were fixed to the universal values when the number of the available experimental data points at the low-density states ($X_{ES} > 0$) is less than 3 for the entire family.
- Finally, component-specific parameters are optimized following criteria reported in Table 2

References

[1] G.M. Kontogeorgis, R. Dohrn, I.G. Economou, J.-C. de Hemptinne, A. ten Kate, S. Kuitunen, M. Mooijer, L.F. Žilnik, V. Vesovic, Industrial Requirements for Thermodynamic and Transport Properties: 2020, Ind. Eng. Chem. Res. 60 (2021) 4987–5013, doi:10.1021/acs.iecr.0c05356.

[2] B.E. Poling, J.M. Prausnitz, J.P. O'Connell, The properties of gases and liquids, 5th ed, McGraw-Hill, New York, 2001.

[3] L.F. Cardona, L.A. Forero, J.A. Velásquez, Correlation and Prediction of Thermal Conductivity Using the Redlich–Kwong Cubic Equation of State and the Geometric Similitude Concept for Pure Substances and Mixtures, Ind. Eng. Chem. Res. 58 (2019) 23417–23437, doi:10.1021/acs.iecr.9b04974.

[4] D. Roy, G. Thodos, Thermal Conductivity of Gases. Organic Compounds at Atmospheric Pressure, Ind. Eng. Chem. Fund. 9 (1970) 71–79, doi:10.1021/i160033a011.

[5] J.F. Ely, H.J.M. Hanley, Prediction of transport properties. 2. Thermal conductivity of pure fluids and mixtures, Ind. Eng. Chem. Fund. 22 (1983) 90–97, doi:10.1021/i100009a016.

[6] M.J. Assael, J.H. Dymond, M. Papadaki, P.M. Patterson, Correlation and prediction of dense fluid transport coefficients. I. n-alkanes, Int. J. Thermophys. 13 (1992) 269–281, doi:10.1007/BF00504436.

[7] S.E. Quiñones-Cisneros, S. Pollak, K.A.G. Schmidt, Friction Theory Model for Thermal Conductivity, J. Chem. Eng. Data. 66 (2021) 4215–4227, doi:10.1021/acs.jced.1c00400.

[8] Y. Rosenfeld, A quasi-universal scaling law for atomic transport in simple fluids, J. Phys. 11 (1999) 5415–5427, doi:10.1088/0953-8984/11/28/303.

[9] G. Galliero, C. Boned, Thermal conductivity of the Lennard-Jones chain fluid model, Phys. Rev. E. 80 (2009) 061202, doi:10.1103/PhysRevE.80.061202.

[10] M. Hopp, J. Gross, Thermal Conductivity of Real Substances from Excess Entropy Scaling Using PCP-SAFT, Ind. Eng. Chem. Res. 56 (2017) 4527–4538, doi:10.1021/acs.iecr.6b04289.

[11] M. Hopp, J. Mele, R. Hellmann, J. Gross, Thermal Conductivity via Entropy Scaling: an Approach That Captures the Effect of Intramolecular Degrees of Freedom, Ind. Eng. Chem. Res. 58 (2019) 18432–18438, doi:10.1021/acs.iecr.9b03998.

[12] M. Hopp, J. Gross, Thermal Conductivity from Entropy Scaling: a Group-Contribution Method, Ind. Eng. Chem. Res. 58 (2019) 20441–20449, doi:10.1021/acs.iecr.9b04289.

[13] H.B. Rokni, J.D. Moore, A. Gupta, M.A. McHugh, R.R. Mallepally, M. Gavaises, General method for prediction of thermal conductivity for well-characterized hydrocarbon mixtures and fuels up to extreme conditions using entropy scaling, Fuel 245 (2019) 594–604, doi:10.1016/j.fuel.2019.02.044.

[14] H.B. Rokni, J.D. Moore, M. Gavaises, Entropy-scaling based pseudo-component viscosity and thermal conductivity models for hydrocarbon mixtures and fuels containing iso-alkanes and two-ring saturates, Fuel 283 (2021) 118877, doi:10.1016/j.fuel.2020.118877.

[15] W.A. Fouad, Thermal Conductivity of Pure Fluids and Multicomponent Mixtures Using Residual Entropy Scaling with PC-SAFT—Application to Refrigerant Blends, J. Chem. Eng. Data. 65 (2020) 5688–5697, doi:10.1021/acs.jced.0c00682.

[16] W.A. Fouad, L.F. Vega, Transport properties of HFC and HFO based refrigerants using an excess entropy scaling approach, J. Supercrit. Fluids 131 (2018) 106–116, doi:10.1016/j.supflu.2017.09.006.

[17] H. Liu, F. Yang, X. Yang, Z. Yang, Y. Duan, Modeling the thermal conductivity of hydrofluorocarbons, hydrofluoroolefins and their binary mixtures using residual entropy scaling and cubic-plus-association equation of state, J. Mol. Liquids 330 (2021) 115612, doi:10.1016/j.molliq.2021.115612.

[18] X. Yang, D. Kim, E.F. May, I.H. Bell, Entropy scaling of thermal conductivity: application to refrigerants and their mixtures, Ind. Eng. Chem. Res. 60 (2021) 13052–13070, doi:10.1021/acs.iecr.1c02154.

[19] W.A. Malatesta, B. Yang, Aviation Turbine Fuel Thermal Conductivity: a Predictive Approach Using Entropy Scaling-Guided Machine Learning with Experimental Validation, ACS Omega 6 (2021) 28579–28586, doi:10.1021/acsomega.1c02934.

[20] S. Chapman, T.G. Cowling, The mathematical theory of non-uniform gases: an account of the kinetic theory of viscosity, thermal conduction, and diffusion in gases, 3rd ed, Cambridge University Press, Cambridge ; New York, 1990.

[21] E. Moine, A. Piña-Martinez, J.-N. Jaubert, B. Sirjean, R. Privat, *I* -PC-SAFT: an Industrialized Version of the Volume-Translated PC-SAFT Equation of State for Pure Components, Resulting from Experience Acquired All through the Years on the Parameterization of SAFT-Type and Cubic Models, Ind. Eng. Chem. Res. 58 (2019) 20815–20827, doi:10.1021/acs.iecr.9b04660.

[22] J.-N. Jaubert, R. Privat, Y.L. Guennec, L. Coniglio, Note on the properties altered by application of a Péneloux-type volume translation to an equation of state, Fluid Phase Equilibria 419 (2016) 88–95, doi:10.1016/j.fluid.2016.03.012.

[23] R. Privat, J.-N. Jaubert, Y.L. Guennec, Incorporation of a volume translation in an equation of state for fluid mixtures: which combining rule? Fluid Phase Equilibria 427 (2016) 414–420, doi:10.1016/j.fluid.2016.07.035.

[24] Y.Le Guennec, S. Lasala, R. Privat, J.-N. Jaubert, A consistency test for α-functions of cubic equations of state, Fluid Phase Equilibria 427 (2016) 513–538, doi:10.1016/j.fluid.2016.07.026.

[25] Y.Le Guennec, R. Privat, S. Lasala, J.-N. Jaubert, On the imperative need to use a consistent α-function for the prediction of pure-compound supercritical properties with a cubic equation of state, Fluid Phase Equilibria 445 (2017) 45–53, doi:10.1016/j.fluid.2017.04.015.

[26] Y.Le Guennec, R. Privat, J.-N. Jaubert, Development of the translated-consistent *tc*-PR and *tc*-RK cubic equations of state for a safe and accurate prediction of volumetric, energetic and saturation properties of pure compounds in the sub- and super-critical domains, Fluid Phase Equilibria 429 (2016) 301–312, doi:10.1016/j.fluid.2016.09.003.

[27] S.K. Mylona, M.J. Assael, W.A. Wakeham, Transport Properties of Fluids, in: Reference Module in Chemistry, Molecular Sciences and Chemical Engineering, Elsevier (2014) B9780124095472110000, doi:10.1016/B978-0-12-409547-2.11001-7.

[28] Experimental Thermodynamics Volume IX, in: M.J. Assael, A.R.H. Goodwin, V. Vesovic, W.A. Wakeham (Eds.)Advances in Transport Properties of Fluids, Royal Society of Chemistry, Cambridge, 2014, doi:10.1039/9781782625254.

[29] G.A. Olchowy, J.V. Sengers, A simplified representation for the thermal conductivity of fluids in the critical region, Int. J. Thermophys. 10 (1989) 417–426, doi:10.1007/BF01133538.

[30] S.B. Kiselev, V.D. Kulikov, Crossover behavior of the transport coefficients of critical binary mixtures, Int. J. Thermophys. 15 (1994) 283–308, doi:10.1007/BF01441587.

[31] R.A. Ferrell, Decoupled-Mode Dynamical Scaling Theory of the Binary-Liquid Phase Transition, Phys. Rev. Lett. 24 (1970) 1169–1172, doi:10.1103/PhysRevLett.24.1169.

[32] A. Eucken, Allgemeine Gesetzmäßigkeiten für das Wärmeleitvermögen verschiedener Stoffarten und Aggregatzustände, Forsch. Ing.-Wes. 11 (1940) 6–20, doi:10.1007/BF02584103.

[33] R. Privat, J.-N. Jaubert, E. Moine, Improving students' understanding of the connections between the concepts of real-gas mixtures, gas ideal-solutions, and perfect-gas mixtures, J. Chem. Educ. 93 (2016) 2040–2045, doi:10.1021/acs.jchemed.6b00553.

[34] Y. Rosenfeld, Relation between the transport coefficients and the internal entropy of simple systems, Phys. Rev. A. 15 (1977) 2545–2549, doi:10.1103/PhysRevA.15.2545.

[35] L. Novak, Self-Diffusion Coefficient and Viscosity in Fluids, Int. J. Chem. React. Eng. 9 (2011), doi:10.1515/1542-6580.2640.
[36] L.T. Novak, Fluid Viscosity-Residual Entropy Correlation, Int. J. Chem. React. Eng. 9 (2011), doi:10.2202/1542-6580.2839.
[37] O. Lötgering-Lin, M. Fischer, M. Hopp, J. Gross, Pure Substance and Mixture Viscosities Based on Entropy Scaling and an Analytic Equation of State, Ind. Eng. Chem. Res. 57 (2018) 4095–4114, doi:10.1021/acs.iecr.7b04871.
[38] O. Lötgering-Lin, J. Gross, Group Contribution Method for Viscosities Based on Entropy Scaling Using the Perturbed-Chain Polar Statistical Associating Fluid Theory, Ind. Eng. Chem. Res. 54 (2015) 7942–7952, doi:10.1021/acs.iecr.5b01698.
[39] I.H. Bell, R. Hellmann, A.H. Harvey, Zero-density limit of the residual entropy scaling of transport properties, J. Chem. Eng. Data. 65 (2020) 1038–1050, doi:10.1021/acs.jced.9b00455.
[40] J.C. Dyre, Perspective: excess-entropy scaling, J. Chem. Phys. 149 (2018) 210901, doi:10.1063/1.5055064.
[41] G. Galliero, Equilibrium, interfacial and transport properties of n-alkanes: Towards the simplest coarse grained molecular model, Chem. Eng. Res. Des. 92 (2014) 3031–3037, doi:10.1016/j.cherd.2014.05.028.
[42] I.H. Bell, R. Messerly, M. Thol, L. Costigliola, J.C. Dyre, Modified Entropy Scaling of the Transport Properties of the Lennard-Jones Fluid, J. Phys. Chem. B. 123 (2019) 6345–6363, doi:10.1021/acs.jpcb.9b05808.
[43] M. Huber, A. Harvey, E. Lemmon, G. Hardin, I. Bell, M. McLinden, NIST Reference Fluid Thermodynamic and Transport Properties Database (REFPROP) Version 10 - SRD 23, (2018). https://doi.org/10.18434/T4/1502528.
[44] M. Dzugutov, A universal scaling law for atomic diffusion in condensed matter, Nature 381 (1996) 137–139, doi:10.1038/381137a0.
[45] Dortmund Data Bank, (2021). www.ddbst.com.
[46] A. Dehlouz, R. Privat, G. Galliero, M. Bonnissel, J.-N. Jaubert, Revisiting the Entropy-Scaling Concept for Shear-Viscosity Estimation from Cubic and SAFT Equations of State: application to Pure Fluids in Gas, Liquid and Supercritical States, Ind. Eng. Chem. Res. 60 (2021) 12719–12739, doi:10.1021/acs.iecr.1c01386.
[47] A. Dehlouz, J. Jaubert, G. Galliero, M. Bonnissel, R. Privat, A new entropy-scaling based model for estimating the self-diffusion coefficients of pure fluids, Ind. Eng. Chem. Res. (2022), doi:10.1021/acs.iecr.2c01086.
[48] DIPPR Data Compilation of Pure Chemical Properties, Design Institute for Physical Properties, (2021). https://dippr.byu.edu.
[49] A. Pina-Martinez, R. Privat, J. Jaubert, Use of 300,000 pseudo-experimental data over 1800 pure fluids to assess the performance of four cubic equations of state: SRK, PR, *tc*-RK, and *tc*-PR, AIChE J. 68 (2022) e17518, doi:10.1002/aic.17518.
[50] N. Ramírez-Vélez, R. Privat, A. Pina-Martinez, J. Jaubert, Assessing the performance of non-associating SAFT-type equations of state to reproduce vapor pressure, liquid density, enthalpy of vaporization, and liquid heat capacity data of 1800 pure fluids, AIChE J. 68 (2022) e17722, doi:10.1002/aic.17722.
[51] P.D. Neufeld, A.R. Janzen, R.A. Aziz, Empirical Equations to Calculate 16 of the Transport Collision Integrals $\Omega^{(l,s)*}$ for the Lennard-Jones (12–6) Potential, J. Chem. Phys. 57 (1972) 1100–1102, doi:10.1063/1.1678363.
[52] L.D. Smoot, D.T. Pratt, Pulverized-Coal Combustion and Gasification: theory and Applications for Continuous Flow Processes,.
[53] I.H. Bell, G. Galliero, S. Delage-Santacreu, L. Costigliola, An entropy scaling demarcation of gas- and liquid-like fluid behaviors, J. Chem. Phys. 152 (2020) 191102, doi:10.1063/1.5143854.
[54] I.H. Bell, S. Delage-Santacreu, H. Hoang, G. Galliero, Dynamic Crossover in Fluids: from Hard Spheres to Molecules, J. Phys. Chem. Lett. 12 (2021) 6411–6417, doi:10.1021/acs.jpclett.1c01594.